

# POWER DIAGRAMS AND MORSE THEORY

D. SIERSMA , M. VAN MANEN

**ABSTRACT.** We study Morse theory of the (power) distance function to a set of points in  $\mathbb{R}^n$ . We describe the topology of the union of the corresponding set of growing balls by a Morse poset. The Morse poset is related to the power tessellation of  $\mathbb{R}^n$ . We remark that the power diagrams from computer science are the spines of amoebas in algebraic geometry, or the hypersurfaces in tropical geometry. We show that there exists a discrete Morse function on the coherent triangulation, dual to the power diagram, such that its critical set equals the Morse poset of the power diagram.

## 1. INTRODUCTION

In this paper we study in a Euclidean space of arbitrary dimension the evolution of a set of balls with fixed centers  $P_1, \dots, P_N$  with respect to increasing radius. Let  $B(P_i, r_i)$  be the ball with center  $P_i$  and radius  $r_i$ . We let all balls grow simultaneously with increasing radius  $r_i = t$ . One can also see this as a set of homogeneous wave fronts that start from the centers with equal (and homogeneous) speed. See figure 1. The space covered by the balls  $B(P_1, t), \dots, B(P_N, t)$  is the set  $B(t) = \bigcup B(P_i, t)$ . We will discuss several aspects of this process:

[T ] (T-Properties) change of topology  $B(t)$  if  $t$  increases.

[G ] (G-Properties) the geometry of the set of points, which are covered for the first time, but exactly by two different balls; to be more precise we get

$$\text{Vor} = \{x \in \mathbb{R}^n \mid \exists i \neq j : d(x, P_i) = d(x, P_j) \leq d(x, P_k) \text{ for all } k\}.$$

This is the well-known *Voronoi diagram* of the Euclidean distance function. Here  $d(x, P_i) = \|x - P_i\|$  is the Euclidean distance from  $x$  to  $P_i$

For the study of T-Properties we will consider Euler characteristic, topological Morse theory, simplicial and cell-complexes and discrete Morse Theory. G-Properties will lead us to Voronoi diagrams, Delaunay tessellations, and the generalizations: power diagrams and power Delaunay tessellations.

There is a second way to describe the union of balls  $B(t)$ . It can be done by the lower level sets of the minimum of the distance functions from a point  $x$  in the Euclidean space to the centers  $P_i$ :

$$d(x) = \min_{i=1, \dots, N} \|x - P_i\|.$$

With this notation  $B(t) = \{x \in \mathbb{R}^n \mid d(x) \leq t\}$ .

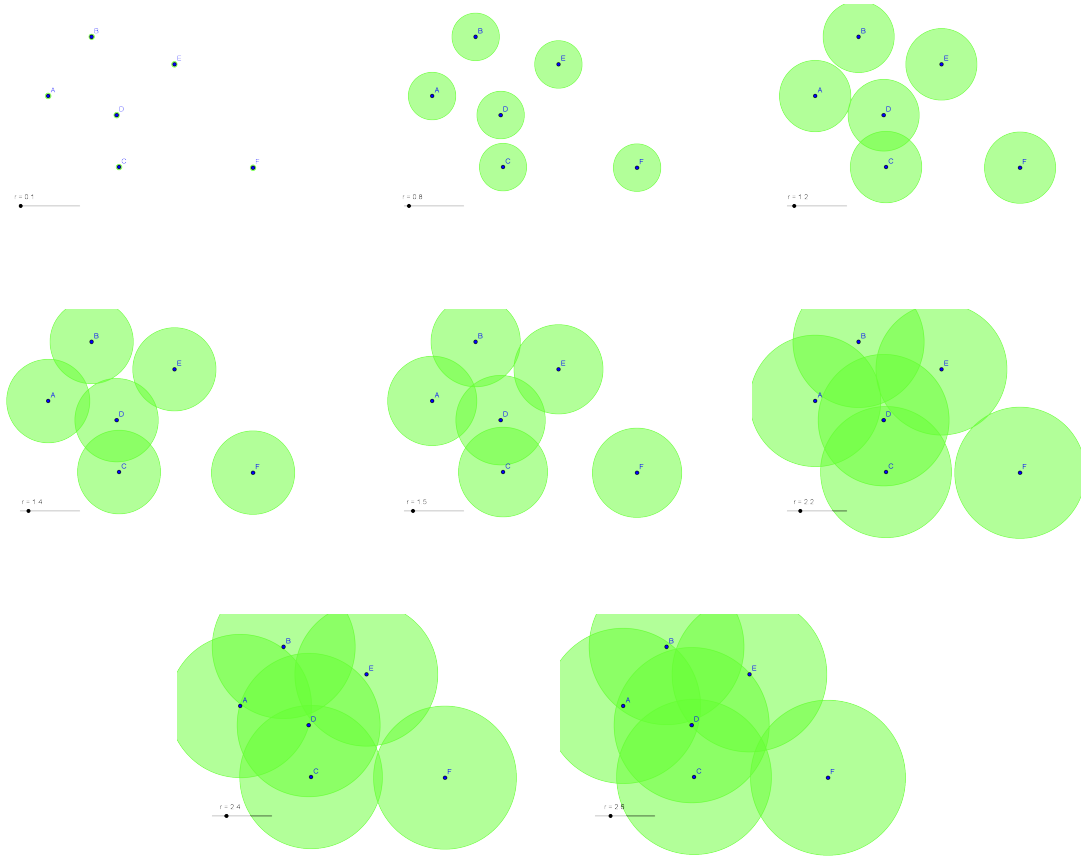


FIGURE 1. Growing balls.

In order to have differentiability in the points of  $\{P_1, \dots, P_N\}$  and to have a nicer formula for the gradient, we study

$$g(x) = \min_{i=1, \dots, N} \frac{1}{2} \|x - P_i\|^2 = \min_{i=1, \dots, N} g_i(x) \text{ where } g_i(x) = \frac{1}{2} \|x - P_i\|^2,$$

which behaves similarly to  $d$ , e.g.  $d$  and  $g$  have the same set of level curves. Note that  $B(\sqrt{2t}) = \{x \in \mathbb{R}^n | g(x) \leq t\}$ .

The evolution of the set of balls will be studied with the (topological) Morse theory of the function  $g : \mathbb{R}^n \rightarrow \mathbb{R}$ . The same scheme can be applied to other distance functions. From section 3 on we will use the so-called power distance function, which generalizes the Euclidean distance.

The paper is organized as follows:

We first describe in section 2 a simple case : points in the plane with Euclidean distance. We use elementary methods (as in [Si]) to study the geometry and topology in order to

give a good an elementary view on what is going on. The treatment in later sections is more abstract and has greater generality (power distance and any dimension).

In section 3 we give the definition of power distance and review properties of the power diagram. This is a tessellation of  $\mathbb{R}^n$  by means of the power distance, which an additively weighted distance function to a point set. A precise definition is given in section 3.

Power diagrams were introduced as a generalization of Voronoi diagrams by Aurenhammer in [Au2]. They play an important role in computational geometry. We will show that power diagrams can also be defined in a second way: by affine functions and as such they occur in algebraic geometry, as the spines of amoebas, see [PR]. Another appearance of the power diagram is what other authors call a tropical hypersurface, see [RST]. They also appear when string theorists use toric geometry, see for instance [DFG]. We spell out the correspondence between the classical theory of Voronoi and power diagrams and that of the spines of amoebas and tropical hypersurfaces. Also the dual of the power diagram, the Delaunay tessellation, plays an important role in the rest of the paper.

In section 4 we study the critical points of the minimum of the power distances to the points  $P_1, \dots, P_N$  and relate it to the Morse poset. This Morse poset is a partial ordered subset, or poset, of the Delaunay tessellation. It encodes the critical points and their Morse types. It turns out that on the complement of the Morse posets there exist a discrete vector field in the sense of Forman.

We present in section 5 the relation between power diagrams and the discrete Morse theory introduced by Forman in [Fo1]. This theory is important, because it describes the order of cell attaching in a combinatorial model for the union of balls  $B(t)$ .

In [Ed3] Edelsbrunner asked to “elucidate the two approaches”. The one being the study of embedded point sets using Euclidean distance functions, and the other one being discrete Morse theory. We solve this in section 6, where we construct a discrete Morse function from Euclidean distance information.

In applications one extensively uses the Morse theory point of view to distinguish between different triangulations of point sets. The Morse poset depends on the metric structure of the point set and can be used as shape classifier. Examples were first given in [SvM] and [Si].

Most of the results in this paper can in some form or another be found in the literature. We tried to include appropriate references in the sections, but in all likelihood we are not complete. New material is contained in section 6, especially theorem 10 and 11.

## 2. TWO DIMENSIONAL CASE, INTUITIVE INTRODUCTION

**2.1. Two dimensional case.** We start with a set of  $N$  different points  $\{P_1, \dots, P_N\}$  in the plane  $\mathbb{R}^2$ . As mentioned above we study the function

$$g(x) = \min_{i=1, \dots, N} \frac{1}{2} \|x - P_i\|^2 = \min_{i=1, \dots, N} g_i(x) \text{ where } g_i(x) = \frac{1}{2} \|x - P_i\|^2,$$

Note that

$$\text{grad } g_i(x) = \text{grad } \frac{1}{2} \|x - P_i\|^2 = \overrightarrow{xP_i}$$

It follows that the set of points where  $g$  is not differentiable is exactly

$$\text{Vor} = \{x \in \mathbb{R}^2 \mid \exists i \neq j : d(x, P_i) = d(x, P_j) \leq d(x, P_k) \text{ for all } k\}.$$

This is the well-known *Voronoi diagram* of the Euclidean distance function  $d$ . The (*closed*) *Voronoi cells* are defined by:

$$\text{Vor}(P_i) = \{x \in \mathbb{R}^2 \mid d(x, P_i) \leq d(x, P_k) \text{ for all } k\}.$$

The two dimensional Voronoi diagrams consist of

- 2-dimensional Voronoi cells,
- 1-dimensional Voronoi edges,
- 0-dimensional Voronoi vertices.

The last two constitute a hypersurface, the Voronoi diagram.

For the theory of Voronoi diagrams we refer to Aurenhammer [Au1], Edelsbrunner [Ed1] and the book of Okabe-Books-Sigihara [OBS]. Voronoi diagrams have many applications in mathematics and computer science, but also in geography, biology, crystallography, marketing, cartography, etc.

The level curves of the squared distance function  $g$  can be considered as *wave fronts*, which start from the points of  $\{P_1, \dots, P_N\}$ . These wave fronts  $\{g = t\}$  bound regions  $\{g \leq t\}$ , where the wave front has already passed, just as a region passed by a forest fire. Each  $\{g \leq t\}$  is a union of balls.

We want to study the change of topology of these regions  $\{g \leq t\}$ . We start with an instructive and very simple example with 3 points, where two different positions of the points of  $\{P_1, P_2, P_3\}$  give rise to different topological behavior. We first consider the simplest indicator for topological changes: the Euler characteristic  $\chi$ .

Consider the level sets in figure 2. Initially the wave fronts surround three different regions. So the Euler characteristic  $\chi = 3$ . We will report changes in  $\chi$  as  $t$  grows. Next, two regions meet in the center of  $P_1P_2$  and we get two contractible regions, so  $\chi = 2$ . After that the third region meets the other (combined) region in the center of  $P_1P_3$ , this gives  $\chi = 1$ .

Next we distinguish two cases:

In case A (figure 2), where one of the angles is *obtuse*, the region becomes bigger and bigger and  $\chi$  does not change anymore.

In case B (figure 2) all the angles are *acute* and now the wave fronts meet once more: in the center of  $P_2P_3$  and enclose a region in the middle of the triangle. The set  $\{g \leq t\}$  forms a cycle and is no longer contractible. Now  $\chi = 0$ . If  $t$  grows further then the enclosed region in the middle disappears and this changes  $\chi$  to 1. A detailed picture is figure 6B. There is only one region left, which is contractible and there are no changes if  $t$  increases further.

We intend to study this type of process in the present paper. The special points where the wave fronts meet and the points where they become non-differentiable are directly related to the Voronoi diagram. As we see in the above example we need more refined information than the Voronoi diagram in order to understand the topological behavior of the wave fronts.

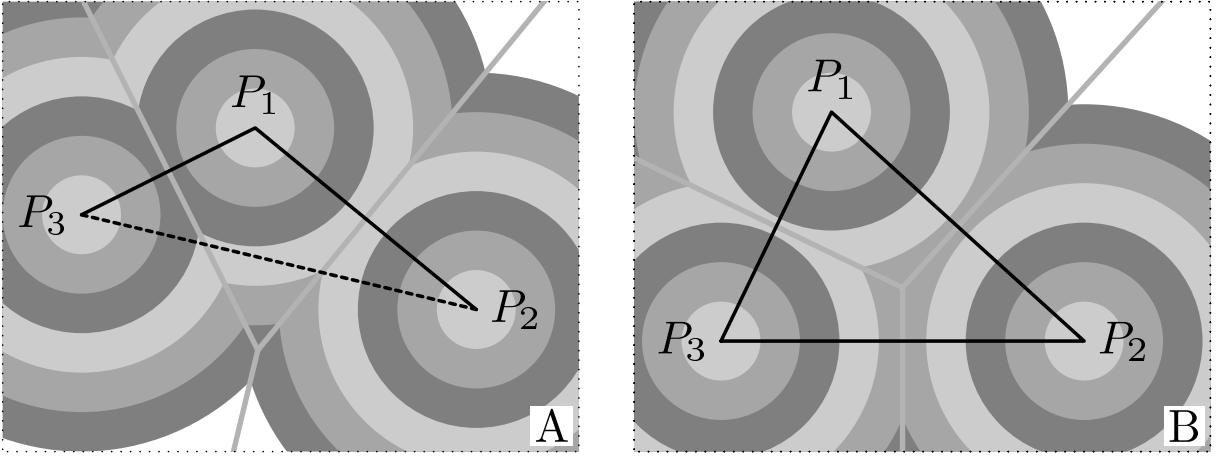


FIGURE 2. Evolution of a wave front from three points, cases A and B

**2.2. Behavior of  $g$  on the plane  $\mathbb{R}^2$ .** The behavior of  $g$  on the *interiors of the Voronoi cells* is clear. In the points of  $\{P_1, \dots, P_N\}$  the function  $g$  has its minimal value and there are no other special points in the interiors of the Voronoi cells. The level curves are there smooth for  $t > 0$ . Next we study the behavior of  $g$  on neighborhoods of the points on the Voronoi diagram: the edges and the vertices.

The edges of the Voronoi diagram are parts of perpendicular bisectors of two points  $P_i$  and  $P_j$ . For an example look at the points  $P_2$  and  $P_3$  in figure 2.

Let  $\text{Vor}(P_2, P_3) = \text{Vor}(P_2) \cap \text{Vor}(P_3)$  be the Voronoi edge between the Voronoi cells of  $P_2$  and  $P_3$ . We will call the perpendicular bisector of the points  $P_2$  and  $P_3$  the separator  $\text{Sep}(P_2, P_3)$  of  $P_2$  and  $P_3$ . Indeed, the perpendicular bisector separates the point  $P_2$  from the point  $P_3$ . Let  $c_{23} = c(P_2, P_3)$  be the midpoint of the segment  $P_2P_3$ :  $c_{23} = \text{Sep}(P_2, P_3) \cap P_2P_3$ .

The edge  $\text{Vor}(P_2, P_3)$  is contained in the separator:  $\text{Vor}(P_2, P_3) \subset \text{Sep}(P_2, P_3)$ . The position of  $c_{23}$  with respect to  $\text{Vor}(P_2, P_3)$  is important. There are three cases (cf. figure 3):

- (1)  $c_{23}$  lies outside  $\text{Vor}(P_2, P_3)$ , the triangle  $\Delta(P_1, P_2, P_3)$  is obtuse. This is case A in figures 2 and 3.
- (2)  $c_{23}$  lies in the interior of  $\text{Vor}(P_2, P_3)$ ,  $\Delta(P_1, P_2, P_3)$  is acute. This is case B in figures 2 and 3.
- (3)  $c_{23}$  is a boundary point of  $\text{Vor}(P_2, P_3)$ ,  $\Delta(P_1, P_2, P_3)$  is right-angled. This is the third case in figure 3.

The position of  $c_{23}$  with respect to  $\text{Vor}(P_2, P_3)$  determines the behavior of  $g$  on  $\text{Vor}(P_2, P_3)$ . In cases (1) and (3)  $g$  is monotone on the edge; in case (2)  $g$  is not monotone, but increasing from  $c_{23}$  in both directions.

Consider a point  $P$  on the *interior of a Voronoi-edge*  $\text{Vor}(P_i, P_j)$ . Suppose first that  $P$  is different from the center of the segment  $P_iP_j$ . Then there is no change in the topology of the lower level sets  $\{g \leq g(P)\}$ , since the set of level curves of  $g$  is topologically

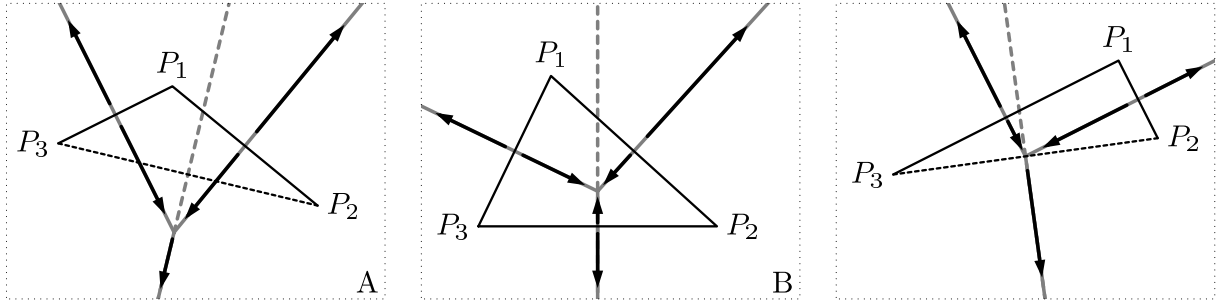


FIGURE 3. Positions of  $c_{23}$  with respect to  $\text{Vor}(P_2, P_3)$ . The gray dashed line is  $\text{Sep}(P_2, P_3)$ . The arrows point to the direction in which  $g$  increases on the Voronoi diagram.

equivalent to a set of parallel lines. More precisely: there exists a homeomorphism  $\phi$  of a open neighborhood of  $P$  onto an open set in  $\mathbb{R}^2$  such that the composed function  $g\phi$  is a linear function. In this case we call  $P$  a *topologically regular point* of  $g$ , see figure 4. Suppose next that  $P$  coincides with the center of the segment  $P_2P_3$ , then it is possible

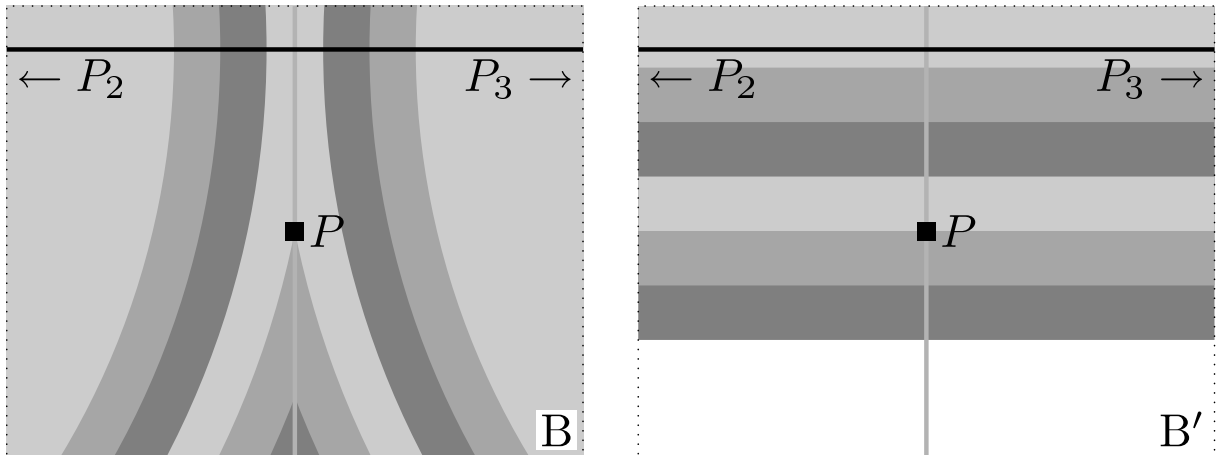


FIGURE 4. Topologically regular situation around  $P$  in picture B. The homeomorphic local change of variables makes the level set look as in picture B'.

to make a non-differentiable (but homeomorphic) change of coordinates  $\phi$ , such that the composed function  $g\phi$  is given by the formula:  $g(P) + x^2 - y^2$ , which defines a differentiable saddle point. In this case we call  $P$  a *topological saddle point* of  $g$  (figure 5).

After having considered neighborhoods of the edges of the Voronoi diagram, the remaining points to consider are the *vertices of the Voronoi diagrams*. At a vertex  $P$  several edges of the Voronoi diagram will meet. We consider the following cases, related to the behavior of the restriction of  $g$  to the edges, containing  $P$ .

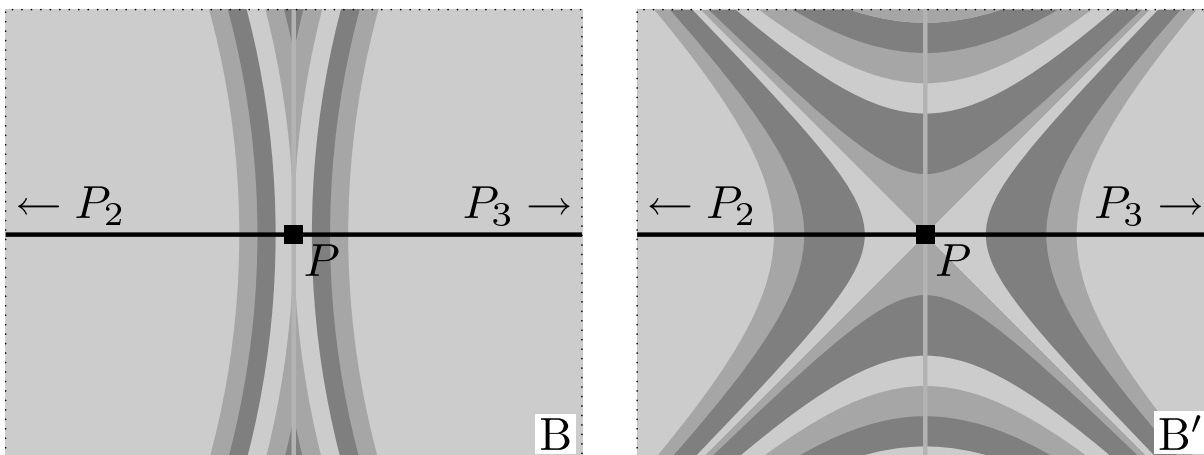


FIGURE 5. At the point  $c(P_2, P_3)$  of example B in figure 2 the function  $g$  has a topological saddle point. The homeomorphic local change of variables makes the level set look as in picture B'.

- i.  $P$  is a maximum of this restriction. We can now use a non-differentiable (but homeomorphic) change of coordinates  $\phi$ , such that the composed function  $g \circ \phi$  is given by the formula:  $g(P) - x^2 - y^2$ , which defines a *local maximum* of  $g$  (figure 6).

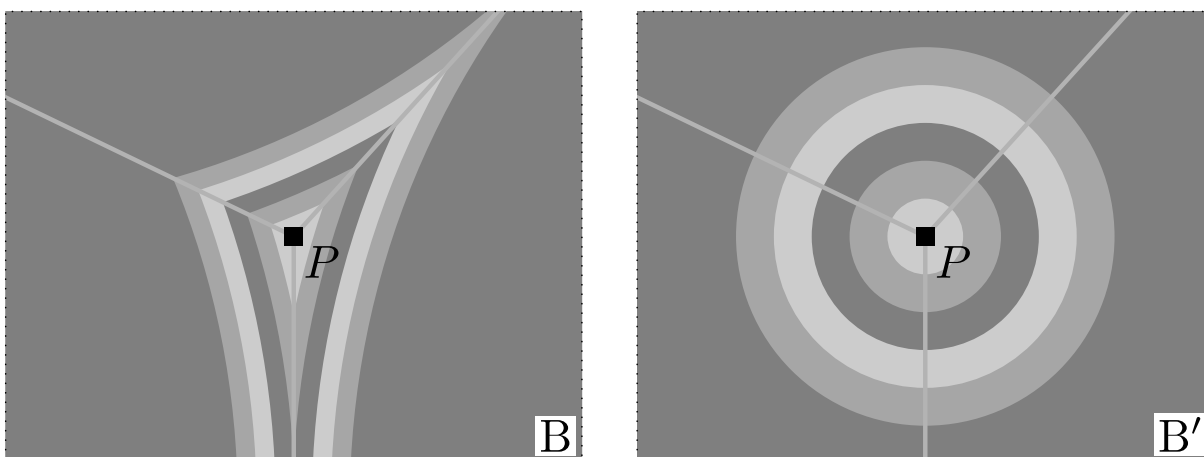


FIGURE 6. A topological maximum

- ii.  $P$  is a maximum on all but one of the adjacent edges. As figure 7 shows in this case there is a non-differentiable (but homeomorphic) change of coordinates that transforms  $g$  into a linear function. Again  $P$  is a *topological regular point* of  $g$ .

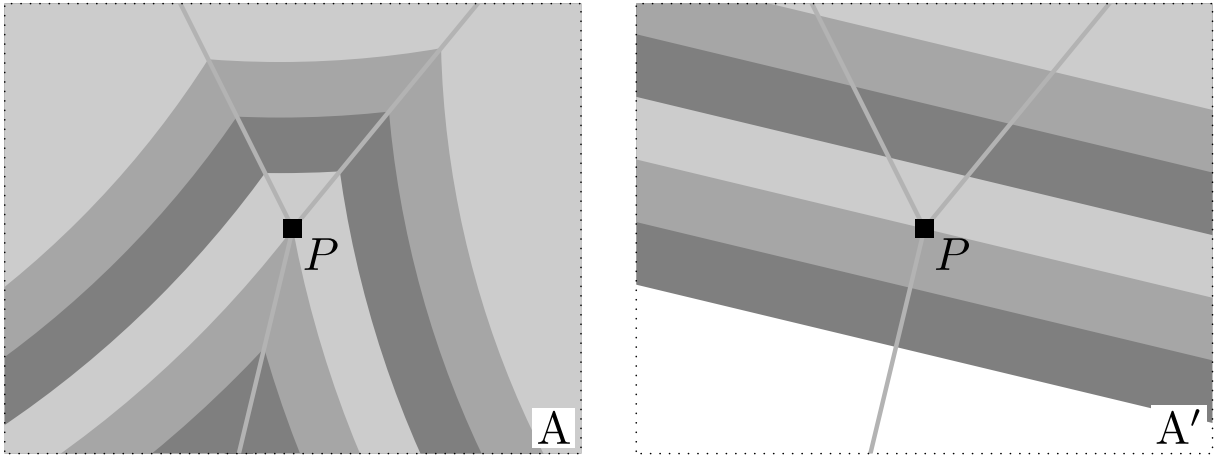


FIGURE 7. A vertex, which is topologically regular

Note that cases other than (i) and (ii) do not exist. The reader may verify this for three adjacent edges. That it holds in other cases ( 4 or more adjacent edges), as well is proved in [Si].

The minima, the saddle points and the maxima of  $g$  are called (topological) critical points of index 0, 1, 2 respectively. They occur as follows:

- a. minima in the centers of the Voronoi cells.
- b. saddle points on the interior of edges of the Voronoi diagram,
- c. maxima, which are vertices of the Voronoi diagram.

but as we have seen not any edge or vertex will give a critical point. We will give a combinatorial criterium in 2.4. The corresponding values are called critical values. The other points are called (topologically) regular. Besides the differentiable regular points in the interior of the Voronoi cells, we will meet also topologically regular points, which lie on the interior of edges of the Voronoi diagram, or are vertices of the Voronoi diagram.

**2.3. Morse formula.** The following Morse formula is a non differentiable version of the 'mountaineering equation'.

**THEOREM 1.** *Let  $s_0$ ,  $s_1$  and  $s_2$  be respectively the number of (topological) minima, saddle points and maxima of the distance functions  $d$  or  $g$ . We have:*

$$s_0 - s_1 + s_2 = 1$$

For the proof one can use the framework of Morse theory, which is well known in differential topology. See Milnor [Mi1] or Hirsch [Hi]. In this article we use topological Morse theory. Morse theory was carried over to the topological case by Morse himself in the articles [Mo1] and [Mo2]. Voronoi diagrams are examples of stratified spaces. Generalizations of Morse theory to stratified spaces by Goresky and MacPherson are discussed in [GM].



For the proof of 1 the main idea is to follow  $\chi\{g \leq t\}$  and to check the formula

$$s_0(t) - s_1(t) + s_2(t) = \chi\{g \leq t\}$$

if  $t$  increases from 0 to infinity. One starts at  $t = 0$  with  $N$  minima only. During the process there are a finite number of values, where  $\chi$  changes with  $-1$  for a saddle point and  $+1$  for a maximum. For  $t$  large enough we have a contractible set, which covers almost  $\mathbb{R}^2$  and  $\chi = 1$  in that case. For more details we refer to [Si].

**2.4. Delaunay tessellation and Morse poset.** The Delaunay tessellation with respect to the point set  $\{P_1, \dots, P_N\}$  is the division of the convex hull  $\text{CH}(\{P_1, \dots, P_N\})$  in polyhedra dual to the Voronoi tessellation of the plane. We now describe how to construct the Delaunay tessellation. The vertices of the *Delaunay tessellation*  $\text{Del}(\{P_1, \dots, P_N\})$  are the points of  $\{P_1, \dots, P_N\}$ . There is an edge connecting two points of  $\{P_1, \dots, P_N\}$  if and only if their Voronoi cells share a common edge (it is not enough that two Voronoi cells intersect only in one point). The 2-simplices are the triangles where 3 (or more) Voronoi cells come together.

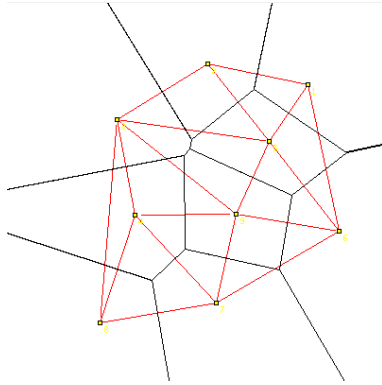


FIGURE 8. Voronoi tessellation and its dual Delaunay tessellation

Note that if the convex hull of  $\{P_1, \dots, P_N\}$  is 2-dimensional and no four points lie on a circle, then the Delaunay tessellation is in fact a triangulation of the convex hull of  $\{P_1, \dots, P_N\}$ . By abuse of language sometimes 'triangulation' is used, where in fact one has only a tessellation.

**Property.** The critical points of our distance function are exactly the intersection points between the Voronoi cells and the corresponding Delaunay cells.

Saddle-points are the intersections of two edges. If the vertex of the Voronoi diagram is contained in the convex hull of the vertices of the corresponding Delaunay cell, then we have a maximum. For any point  $P_i \in \{P_1, \dots, P_N\}$  the Voronoi and Delaunay cell intersect in the point itself. Indeed all the points  $P_i$  are minima of the distance function.

So to each critical point there belongs a cell in the Delaunay tessellation, which we call *active* or *critical*. These active cells constitute a poset: the Morse poset. Note that the Morse poset is in general not a simplicial complex. It is only a poset. Recall that a poset

is a set with a partial order. In this case the partial order is inclusion. The Morse poset is a subset of the Delaunay tessellation.

It was shown in [SvM] that the Morse poset is a useful shape classifier. Its 1-skeleton was called in [Si] the *saddles-maxima graph* of  $\{P_1, \dots, P_N\}$ , for short  $\text{sm}(\{P_1, \dots, P_N\})$  (cf. figures 9 and 24). This saddles-maxima graph is known in computer science as the

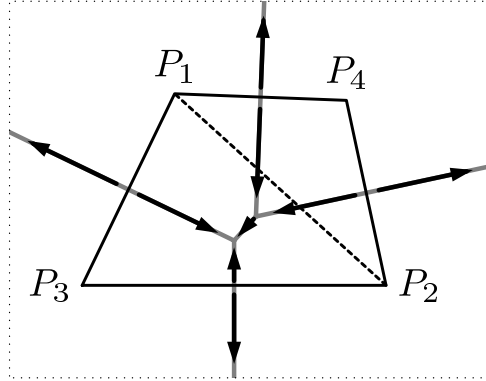


FIGURE 9. Saddles-maxima graph.

*Gabriel graph*, cf. [GS] and [Ur]. We leave it to the reader to show that in fact the saddles-maxima graph  $\text{sm}$  is connected.

**2.5. Next to a discrete Morse function.** To the Morse poset we can add extra information about the topological cell attaching: just give a cell of the Delaunay tessellation the value of the distance function  $g$  at the corresponding critical point. We call this a discrete function on the Morse poset.

This is near to the concept of discrete Morse theory, which we will describe in section 5. The starting point there is a function on the simplices of a simplicial complex. In our case we could take the Delaunay tessellation and extend the discrete function with values on the simplices which are not in the Morse poset.

One can do this as follows in the (above) two 3-points examples :

- Acute triangle. All cells belong to the Morse poset.
- Obtuse triangle. The three vertices and two of the edges belong to the Morse poset; assigne to the third edge and the 2-simplex the maximal value of  $g$  on each of them (they turn out to be equal).

In more complicated examples: follow the same strategy. Add a missing 2-cell together with a boundary 1-cell as soon as the two other boundaries are attached (give a value slightly higher, but lower than the next critical value).

We will treat this in more detail in section 6. In theorem 10 we discuss the extension to a discrete Morse function in all dimensions. Discrete Morse functions are easy to implement on computers and in this case they carry a lot of information about “shape”.

3. POWER DIAGRAMS AND TROPICAL HYPERSURFACES.

In this section we show the equivalence of two definitions of the power diagram. First we discuss the original notion of Aurenhammer, by means of the power distance function, as used in computational geometry. Then we show that these are equivalent to the definitions by means of affine functions, as used in algebraic geometry. Note that we avoid genericity conditions in the treatment below.

**3.1. The definition of Aurenhammer.** Take a point set  $\{P_1, \dots, P_N\} \subset \mathbb{R}^n$ . Throughout this article we assume that  $\dim(\text{CH}(\{P_1, \dots, P_N\})) = n$ . Assign a weight  $w_i$  to each point  $P_i$ . Then write down the functions:

$$(1) \quad g_i: \mathbb{R}^n \rightarrow \mathbb{R} \quad g_i(x) = \frac{1}{2}\|x - P_i\|^2 - \frac{1}{2}w_i \quad g(x) = \min_{1 \leq i \leq N} g_i(x)$$

Here we have used the following notation:

$$\|x\|^2 = \sum_{i=1}^n x_i^2$$

Note that  $2g_i(x)$  is equal to the the square of the tangent from the point  $x$  to the sphere around  $P_i$  with radius  $r_i = \sqrt{w_i}$  (as soon as  $x$  is outside that sphere). This value is in Euclidean geometry known as the power of a point with respect to that sphere. Points on the sphere have 2

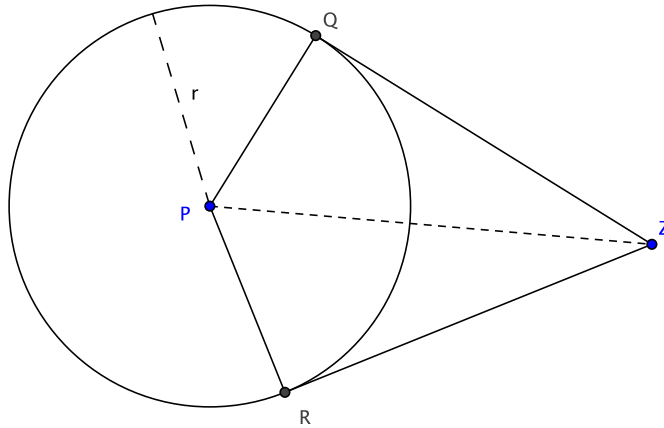


FIGURE 10. Power of a point with respect to a sphere

**DEFINITION 1.** For a subset  $\alpha \subset \{P_1, \dots, P_N\}$  the set  $\text{Pow}(\alpha)$  is the closure of

$$\{x \in \mathbb{R}^n \mid g_i(x) = g(x) \ P_i \in \alpha \text{ and } g_j(x) > g(x) \ P_j \notin \alpha\}$$

The sets  $\text{Pow}(\alpha)$  are called (power) cells.

It is no restriction to assume that  $w_i > 0$ . We may add some number to all of the functions  $g_i$ : the cells will not change. In fact we can add any function  $h: \mathbb{R}^n \rightarrow \mathbb{R}$  to the  $g_i$ . We will get the same power cells.

We repeat definition 1 in [PR].

**DEFINITION 2.** A polyhedral subdivision ( resp. polytopal subdivision )  $\mathcal{T}$  of a polyhedron  $K \subset \mathbb{R}^n$  is a subdivision of  $K$  in polyhedra ( resp. polytopes )  $K_i$ , such that

- The union of all sets  $K_i \in \mathcal{T}$  is  $K$ .
- If  $K_i$  and  $K_j$  are both in  $\mathcal{T}$  then so is their intersection.
- Every compact subset  $L$  of  $K$  intersects only a finite number of the  $K_i$ .

**THEOREM 2.** The sets  $\text{Pow}(\alpha)$  for  $\alpha \subset \{P_1, \dots, P_N\}$  are a polyhedral subdivision of  $\mathbb{R}^n$ . This polyhedral subdivision is called the power diagram.

*Proof.* The cells cover  $\mathbb{R}^n$ . They are the intersection of a finite number of half spaces of the form:  $\{x \in \mathbb{R}^n \mid g_i(x) \leq g_j(x)\}$ . So they are polyhedra.  $\square$

Besides many similarities , there are at least two differences between power diagrams and Voronoi diagrams.

- In a power diagram the cell of a point may well be empty. It might happen that for some  $i$  there is for every  $x \in \mathbb{R}^n$  a  $j = j(x, i)$  such that  $g_j(x) < g_i(x)$ .
- Whereas in Voronoi diagrams,  $P_i$  is always contained in its own cell, in a power diagram the cell of  $P_i$  might not be empty and still  $P_i$  does not lie in its own cell.

We will see instances of these two phenomena in the examples below.

Recall that the Voronoi diagram can be constructed using the upper convex hull to the tangent planes to a parabola  $x_0 = \frac{1}{2} \sum_{i=1}^n x_i^2$  at the points  $\{P_1, \dots, P_N\}$ . For power diagrams a similar construction exists. Look at figure 11. We take cylinders with radius  $r_i = \sqrt{w_i}$  around the lines  $x = P_i$  in  $\mathbb{R}^{n+1}$ . The intersection of the cylinders with the parabola lies in a hyperplane. We draw the hyperplanes in which they lie ( left figure ) and we consider the upper convex hull of these hyperplanes (right figure). The projection of its singular sides is the power diagram.

The above construction is described in [Au2], section 4.1. When the  $r_i = 0$  the construction reduces to the well-known construction of Voronoi diagrams. In that case, of course, one has to take the tangent planes to the paraboloid.

**3.2. Digression on Tropical Geometry.** We will connect the theory of power diagrams with the concept of tropical hypersurface in tropical geometry. For this purpose we make a short digression on this subject. For surveys on the subject we refer to [RST] and [Ga].

Tropical geometry is a relatively new development in algebraic geometry that tries to connect algebraic geometry problems with combinatorial questions on certain polytopes. Recall that algebraic geometry studies varieties: the zero set of polynomials with real or complex coefficients in affine space.

In tropical geometry one considers two new operations in  $\mathbb{R}$ :

- tropical addition:  $x \oplus y := \min(x, y)$ , and
- tropical multiplication:  $x \otimes y := x + y$ .

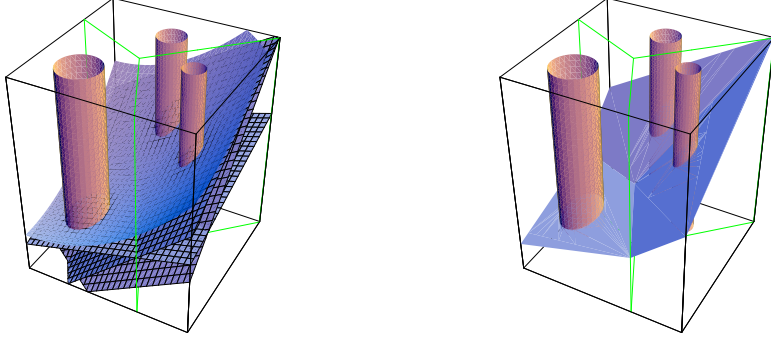


FIGURE 11. Power lifting to the parabola

With these two operations  $\mathbb{R}$  gets the structure of a topological semi-ring. Such a tropical semi-ring is called a *min-plus algebra*.

Polynomials in tropical geometry are defined in the usual way. The “dictionary” from algebraic geometry to tropical geometry works as follows: The ordinary polynomial

$$4x^3 + 4y^3 + 2xy + 7$$

has a tropical version:

$$\min\{3x + 4, 3y + 4, x + y + 2, 7\}.$$

Tropical polynomials are piecewise linear concave functions on  $\mathbb{R}^n$  with integer coefficients. They come together with a vertex set defined by the exponents; in the example  $(3, 0)$ ,  $(0, 3)$ ,  $(1, 1)$ ,  $(0, 0)$ .

The analogue of a variety in tropical geometry is the non-differentiability locus of the tropical polynomial, also called the corner locus of the concave function. A corner locus is drawn in figure 12.

The pictures one gets look similar to power diagrams. Also tessellations of the polytope of the vertex set appear in a natural way in tropical geometry.

Because of the relation  $\max(x, y) = -\min(-x, -y)$  one could also have used the operation  $x \oplus y = \max(x, y)$  to define a tropical semi-ring. Tropical hypersurfaces are in that context piecewise linear convex functions. We will use this convention in the rest of this paper.

The remarkable fact is that these tropical hypersurfaces also appear in a very different way.

Let  $V \subset (\mathbb{C}^*)^n$  be an algebraic variety. Recall that  $\mathbb{C}^* = \mathbb{C} - 0$  is the group of complex numbers under multiplication. Let  $\text{Log}: (\mathbb{C}^*)^n \rightarrow \mathbb{R}^n$  be the “logarithmic moment-map” defined by

$$\text{Log}(z_1, \dots, z_n) = (\log|z_1|, \dots, \log|z_n|).$$

Gelfand-Kapranov-Zelevinski defined the *amoeba* of an algebraic variety  $V$  as the image  $A = \text{Log}(V) \in \mathbb{R}^n$ . As one can see in the articles [PR], [Ga] and elsewhere that the

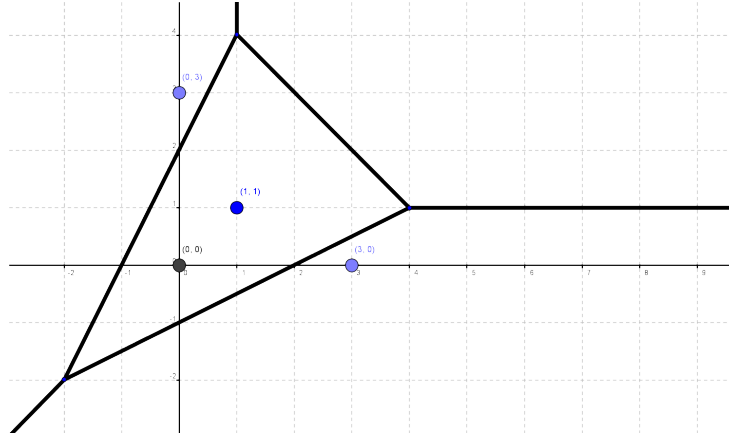


FIGURE 12. The corner locus for  $\min\{3x + 4, 3y + 4, x + y + 2, 7\}$ .

tropical hypersurfaces (drawn with the maximum convention) are “spines” of amoebas of algebraic varieties. It is a deep result in tropical geometry established by Mikhalkin that



FIGURE 13. Amoeba of  $3x^2 + 5xy + y^3 + 1$

the spine is a certain limit of the amoeba and carries all topological information of the amoeba.

For details we refer the interested reader to [RST], [Ga], [GKZ] and [Ga].

**3.3. Power diagram as tropical hypersurface.** As we hinted at in the previous section the power diagram can also be defined using only affine functions. Let as in equation (1):

$$g_i(x) = \frac{1}{2}\|x - P_i\|^2 - \frac{1}{2}w_i \quad g(x) = \min_{1 \leq i \leq N} g_i(x)$$

Take the affine functions  $f_i(x) = \langle x, P_i \rangle + c_i$ , where the coefficient  $c_i$  is

$$(2) \quad c_i = -\frac{\|P_i\|^2 - w_i}{2}$$

Consider the maximum of the  $f_i$ :

$$f(x) = \max_{i=1, \dots, N} f_i(x)$$

Then  $f$  and  $g$  satisfy the following relations:

$$(3) \quad g_i(x) = \frac{1}{2}\|x\|^2 - f_i(x) \quad g(x) = \frac{1}{2}\|x\|^2 - f(x)$$

The relations in equation (3) show that we can define the power diagram solely using affine functions.

**PROPOSITION 1.** *For a subset  $\alpha \subset \{P_1, \dots, P_N\}$  the set  $\text{Pow}(\alpha)$  is the closure of*

$$\{x \in \mathbb{R}^n \mid f_i(x) = f(x) \ P_i \in \alpha \text{ and } f_j(x) < f(x) \ P_j \notin \alpha\}$$

Using the affine definition it is immediate that the following two statements that are false for Voronoi diagrams are true for power diagrams. These two statements can also be found in [Au2].

**PROPOSITION 2.** *The intersection of a hyperplane with a power diagram is again a power diagram. The image of a power diagram under an affine map  $\mathbb{R}^n \rightarrow \mathbb{R}^n$  is again a power diagram.*

So a power diagram can be sliced, after which we obtain a new power diagram. In fact, every power diagram in  $\mathbb{R}^n$  is a slice of a Voronoi diagram in  $\mathbb{R}^{n+1}$ .

**PROPOSITION 3.** *Let  $\mathcal{T}$  be a power diagram in  $\mathbb{R}^n$ . There is a Voronoi diagram  $\Upsilon$  in  $\mathbb{R}^{n+1}$  and a hyperplane  $H$  such that  $H \cap \Upsilon = \mathcal{T}$ .*

*Proof.* We will explicitly construct such an  $\Upsilon$ . Let  $\{P_1, \dots, P_N\}$  be the set of points in  $\mathbb{R}^n$  that determine  $\mathcal{T}$ . Write in  $\mathbb{R}^{n+1}$ :

$$Q_i = (P_i, P'_i) \quad \bar{x} = (x, x')$$

We have

$$\|\bar{x} - Q_i\|^2 = \|x - P_i\|^2 + (x' - P'_i)^2$$

So when  $x' = 0$  we get

$$\|\bar{x} - Q_i\|^2 = \|x - P_i\|^2 + P_i'^2$$

Now let the power diagram be given by functions  $g_i$  as in equation (1). It is no restriction to assume that  $w_i < 0$ , because only the differences  $w_i - w_j$  matter for the power diagram. Thus we can choose  $P'_i = \sqrt{-w_i} = r_i$ .  $\square$

**3.4. The Legendre transform.** In the 2-dimensional case we saw that the Delaunay tessellation is the dual of the Voronoi diagram. In a similar way there exists in any dimension a dual of the power diagram. Using the tropical point of view ( with affine functions ) we can best explain the dual object using the Legendre transform, see [Hö], which we explain below. This dual object is also considered in [GKZ], where it has the name *coherent triangulation*.

We start with some definitions. Let  $P$  be a polyhedron in  $\mathbb{R}^{n+1}$ . Let  $v$  be a vector in  $\mathbb{R}^n$ . The *lower faces* of  $P$  with respect to  $v$  are those faces  $F$  of  $P$  such that

$$\forall x \in F \quad \forall \lambda \in \mathbb{R}_{>0}: x - \lambda v \notin P$$

A polytopal subdivision of a polytope in  $\mathbb{R}^n$  is called *coherent* if it is the projection of the lower faces of a polytope in  $\mathbb{R}^{n+1}$ . Not every polyhedral subdivision is coherent, see chapter 5 in [Zi], or chapter 7 in [GKZ].

**DEFINITION 3.** *The Legendre transform of a convex function  $f$ , with domain  $D \subset \mathbb{R}^n$  is*

$$\hat{f}(\xi) = \sup_{x \in D} (\langle \xi, x \rangle - f(x))$$

When the supremum does not exist, we put  $\hat{f}(\xi) = \infty$ . The domain  $\text{Dom}(\hat{f})$  of  $\hat{f}$  are those  $\xi$  for which  $\hat{f}(\xi) < \infty$ .

The Legendre transform of  $f(x) = \frac{1}{2}\|x\|^2$  is the function itself. The Legendre transform of a linear function  $f_i = \langle x, P_i \rangle + c_i$  is  $< \infty$  only when  $\xi = P_i$ . Theorem 2.2.7 of [Hö] reads:

**THEOREM 3.** *Let  $f = \sup_{\alpha \in A} f_\alpha(x)$  be the maximum of a number of lower semi-continuous convex functions. Then  $f$  is also a lower semi-continuous convex function. Furthermore  $\hat{f}$  is the infimum over all finite sums:*

$$\hat{f}(\xi) = \inf_{\sum \lambda_\alpha \xi_\alpha = \xi, \lambda_\alpha > 0, \sum \lambda_\alpha = 1} \sum \lambda_\alpha \hat{f}_\alpha(\xi_\alpha)$$

With theorem 3 we calculate next the Legendre transform of the function that determines the power diagram. We have

$$f = \max_{1 \leq i \leq N} \langle x, P_i \rangle + c_i$$

The domain where  $\hat{f} < \infty$  is the convex hull of the points  $\{P_1, \dots, P_N\}$ . We have

$$\hat{f}_i(P_i) = -c_i \Rightarrow \hat{f}(\xi) = \inf \left( - \sum_i \lambda_i c_i \right)$$

where the infimum is taken over all  $\lambda_i$  such that

$$\sum_{1 \leq i \leq N} \lambda_i P_i = \xi \quad \text{and} \quad \forall i: \lambda_i \geq 0 \quad \text{and} \quad \sum_{i=1}^N \lambda_i = 1$$

It is no restriction to assume that not more than  $n+1$  of the  $\lambda_i$  are non-zero because any point in the convex hull of the  $P_i$  can be expressed as a sum of  $\dim \text{CH}(\{P_1, \dots, P_N\})$  of the  $P_i$ . The infima are best thought of in a geometric way. Take the convex hull  $\text{CH}(\{(P_i, -c_i)\}_{i=1}^N)$ . The lower faces form the graph of  $\hat{f}$  over the convex hull  $\text{CH}(\{P_1, \dots, P_N\})$ . We summarize our discussion in a theorem, that can also be found in [GKZ].



**THEOREM 4.** *Let  $\mathcal{T}$  be a power diagram. Let  $\Upsilon$  be the lower convex hull of the lifted points  $(P_i, -c_i)$  wrt. to the vector  $(0, \dots, 0, 1)$ . The polyhedral complex  $\Upsilon$  is the graph of the Legendre transform  $\hat{f}$  of  $f$ . The domain  $\text{Dom}(\hat{f})$  of  $\hat{f}$  is the convex hull  $\text{CH}(\{P_1, \dots, P_N\})$ .*

The geometrical construction is directly related to the construction of figure 11. If we put the upper convex hull of theorem 4 in figure 11 we get figure 14. What exactly

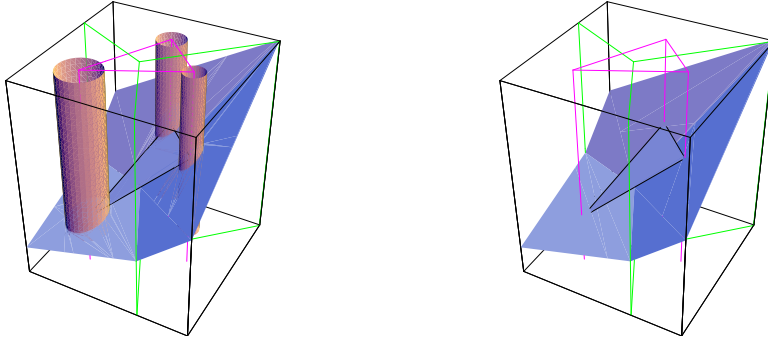


FIGURE 14. The power lift and the Legendre transform

happens here can best be understood by writing out the equations. In figure 11 the graph of  $x_0 = \frac{1}{2}\|x\|^2$  is drawn. Then the cylinders in the picture are  $\|x - P_i\|^2 = r_i^2$ . Or  $\|x - P_i\|^2 = w_i$ . Hence the three planes of which we determine the upper hull are

$$(4) \quad x_0 = \langle x, P_j \rangle + \frac{r_j^2 - \|P_j\|^2}{2}$$

The triangle in figure 14 is the plane  $x_0 = -\sum \lambda_i c_i$  where the  $\lambda_i$  are defined by  $x = \sum \lambda_i P_i$ . In the point  $P_i$  we have that the graph of  $f(x) = \max_i f(x)$  lies  $\frac{w_i}{2}$  above the paraboloid  $x_0 = \frac{1}{2}\|x\|^2$ , whilst the graph of  $\hat{f}(\xi)$  lies  $\frac{w_i}{2}$  below the paraboloid there.

Theorem 4 gives a dual coherent triangulation of the power diagram.

**DEFINITION 4.** *Given a power diagram  $\mathcal{T}$  specified by  $N$  affine functions on  $\mathbb{R}^n$ , the coherent triangulation or (power) Delaunay tessellation of  $\{P_1, \dots, P_N\}$  is the division of  $\text{CH}(\{P_1, \dots, P_N\})$  into polytopes bounded by the set of points  $\xi \in \text{CH}(\{P_1, \dots, P_N\})$  where  $\hat{f}$  is not differentiable.*

Since the coherent triangulation is the projection of the lower convex hull, it is immediate that the sets bounded by the corner locus are in fact polytopes. We will use ‘coherent triangulation’ in relation with affine functions and ‘(power) Delaunay tessellation’ in relation to the quadratic power distance. We also will omit ‘power’. In the case when all the weights  $w_i$  are zero this coherent triangulation is of course the (classical) Delaunay tessellation.

We next discuss some general position arguments. A number of points in  $\{P_1, \dots, P_N\}$  in  $\mathbb{R}^n$  is affinely in general position when the convex hull of each subset of length  $n + 1$

of  $\{P_1, \dots, P_N\}$  is full dimensional. For Voronoi diagrams it might still be that  $n + 2$  lie on a sphere. In that case the Delaunay tessellation is not a simplicial complex. As condition for the (classical) Delaunay tessellation to really be a triangulation we need that the points  $\{Q_1, \dots, Q_N\}$  are affinely general position in  $\mathbb{R}^{n+1}$  where  $Q_i = (P_i, \frac{1}{2}\|P_i\|^2)$ .

**DEFINITION 5.** *A power diagram  $f = \max f_i$  is in general position when the points  $Q_i$  are affinely in general position in  $\mathbb{R}^{n+1}$ . Here*

$$Q_i = (P_i, -c_i), \quad 1 \leq i \leq N$$

The following theorem is left to the reader.

**THEOREM 5.** *The Delaunay tessellation is a simplicial complex when the power diagram is in general position.*

We can combine  $f$  and  $\hat{f}$  in the following function:

$$(\xi, x) \mapsto F(x, \xi) = f(x) + \hat{f}(\xi) - \langle x, \xi \rangle$$

The function hides the Gateau differential of  $f$ . Namely let  $h: \mathbb{R}^n \rightarrow \mathbb{R}$  be a function. If the limit

$$h'(x; \xi) = \lim_{t \downarrow 0} \frac{h(x + t\xi) - h(x)}{t}$$

exists, it is called the Gateau differential. See [Hö], theorem 2.1.22. For a convex set  $K \subset \mathbb{R}^n$  the *supporting function* of  $K$  is the function

$$\xi \mapsto \sup_{x \in K} \langle x, \xi \rangle$$

Theorem 2.2.11. in [Hö] says that the Gateau differential  $\xi \rightarrow f'(x; \xi)$  is the supporting function of the set  $\delta f(x)$  where

$$\delta f(x) = \{\mu \mid F(x, \mu) = 0\}$$

Let us see what that means. Take  $\xi$  to be one of the points of  $\{P_1, \dots, P_N\}$ . Then  $\hat{f}(P_i) = -c_i$ . So the set of  $x$  where  $F(x, \xi) = 0$  are those for which  $f(x) = \langle x, P_i \rangle + c_i$ .

The Gateau differential is called Clarke's generalized derivative in [APS]. It is stated in that article that  $\partial f(x)$  is the convex hull of the gradients of the functions  $f_i$  for which  $f_i(x) = f(x)$ . Let  $\alpha$  be the set of points such that  $f(x) = f_i(x) \Leftrightarrow P_i \in \alpha$ . So  $x \in \text{Pow}(\alpha)$ . Note moreover that these gradients are  $\overrightarrow{xP_i}$ . So we get the convex hull of the points of  $\alpha$ , which is  $\text{Del}(\alpha)$ .

That last statement and the theorem 2.1.22 [Hö] are all equivalent to what is neatly formulated in proposition 1 of [PR]:

**THEOREM 6.** *There is a subdivision of the convex hull  $\text{CH}(\{P_1, \dots, P_N\})$ , dual to the power diagram  $\mathcal{T}$ . The cell  $\text{Del}(\alpha)$  dual to  $\text{Pow}(\alpha) \in \mathcal{T}$  is*

$$\text{Del}(\alpha) = \{\xi \mid F(x, \xi) = 0 \quad \forall x \in \text{Pow}(\alpha)\}$$

*Reverseely*

$$\text{Pow}(\alpha) = \{x \mid F(x, \xi) = 0 \quad \forall \xi \in \text{Del}(\alpha)\}$$

**REMARK 1.** *One should make a difference between the Delaunay tessellation in the abstract sense, as subsets  $\alpha$  of  $\{P_1, \dots, P_N\}$ , and its geometric realization  $\text{Del}(\alpha)$ . But in several cases, where we expect no confusion, we will not distinguish between the two. So if  $\alpha \subset \beta$  then we may say both ‘ $\alpha$  is a face of  $\beta$ ’ or ‘ $\text{Del}(\alpha)$  is a face of  $\text{Del}(\beta)$ ’. Remark that (by duality) the power tessellation is given by the same set of subsets of  $\{P_1, \dots, P_N\}$ , but with a different geometric realization by  $\text{Pow}(\alpha)$ , which has complementary dimension.*

#### 4. THE MORSE POSET

**4.1. Introduction.** In section 2 we studied in 2 dimensions the evolution of a set of wave fronts from a point set: growing discs with equal radius. We discussed critical points, the corresponding Morse poset, the changes in topology and the relation with Voronoi and Delaunay tessellations. In this section we generalize to power distance functions. The corresponding Morse theory concerns the evolution of a set of growing balls in  $n$ -space with different radii. The union of fixed set of balls occur in models of molecules and are studied by e.g. Edelsbrunner [Ed2]. A related approach via alpha-shapes in  $\mathbb{R}^3$  can be found in [DGJ], [GJ1] and [GJ2]. Further related developments are in [CL].

Let us remark here that the topology of level sets of distance functions has been studied before with classical results that are not restricted to a finite set of points. In Riemannian geometry see for example [Gr] and [Ch]; in non-smooth analysis [Cl] and more recently in shape reconstruction [CL]. We will use also the theory of continuous selections [APS].

We will define next Morse critical points in context of continuous functions. For topological Morse theory we refer to [Mo1].

**DEFINITION 6.** *Two functions  $f_1: U_1 \rightarrow \mathbb{R}$  and  $f_2: U_2 \rightarrow \mathbb{R}$  are called topologically equivalent if there exist a homeomorphism  $\phi: U_1 \rightarrow U_2$  such that  $f_1 = f_2 \circ \phi$ . A function  $f: M \rightarrow \mathbb{R}$  is topologically regular at  $x \in M$  if there exists a neighborhood  $U$  of  $x$  such that the restriction  $f|_U$  is topologically equivalent to a linear function. A point  $x$  is called a critical point of  $f$  if  $f$  is not topologically regular at  $x$ . The critical point is called topologically isolated if there exists a neighborhood  $U$  of  $x$  such that all points  $y \in U, y \neq x$  are regular points of  $f$ . A topologically isolated critical point  $x$  of  $f: M \rightarrow \mathbb{R}$  is a topological Morse point of index  $d$  if there exists a neighborhood  $U$  of  $x$  such that the restriction  $f|_U$  has the property that for  $\epsilon$  small enough the set  $\{x \in M \mid f(x) \leq x + \epsilon\}$  is homotopy equivalent to  $\{x \in M \mid f(x) \leq x - \epsilon\} \cup d$ -cell.  $f$  is called a topological Morse function if all critical points are topological Morse.*

**EXAMPLE 1.** *Standard examples  $f: \mathbb{R}^n \rightarrow \mathbb{R}$  are*

- *classical Morse point; [Mil]:*  

$$f(x) = -(x_1^2 + \dots + x_d^2) + (x_{d+1}^2 + \dots + x_n^2)$$
- *Morse point of continuous selections; [APS]:*  

$$f(x) = \min(x_1, \dots, x_d, -(x_1 + \dots + x_d)) + (x_{d+1}^2 + \dots + x_n^2)$$

We will omit the adjective “topologically” in the sequel and simply write: regular point, Morse point, and so on.

4.2. **Critical points of the power distance function  $g$ .** Consider again the function

$$g(x) = \min_{1 \leq i \leq N} g_i(x)$$

Critical points  $x$  of  $g$  are related to the generalized derivative  $\partial g(x)$ . For this concept and related notions we refer to [Cl]. Let  $x$  be a point of the power diagram; then there is a set  $\alpha$  such that

$$(5) \quad g(x) = g_i(x) \Leftrightarrow P_i \in \alpha$$

So  $x \in \text{Pow}(\alpha)$ . Note that  $\text{grad } g_i(x) = x - P_i = \overrightarrow{xP_i}$ . The generalized derivative  $\partial g(x)$  is the convex hull in the vector space  $\mathbb{R}^n$  of the end points of the gradient vectors, so  $\partial g(x) = \text{CH}(\overrightarrow{xP_i})$ . By an affine transformation (sending the origin to  $x$ ) one can identify  $\partial g(x)$  with  $\text{CH}(\alpha) = \text{Del}(\alpha)$ .

Analogously to what was done in 2.2 there are now three cases to consider:

**Inside**  $0 \in \text{Interior}(\partial g(x))$ , hence:  $x$  lies in  $\text{Interior}(\text{CH}(\alpha))$ , or

**Outside**  $0 \notin \partial g(x)$ , hence:  $x$  lies outside  $\text{CH}(\alpha)$ , or

**Border**  $0$  lies on the relative border of  $\partial g(x)$ , hence  $x$  lies on the border of  $\text{CH}(\alpha)$ .

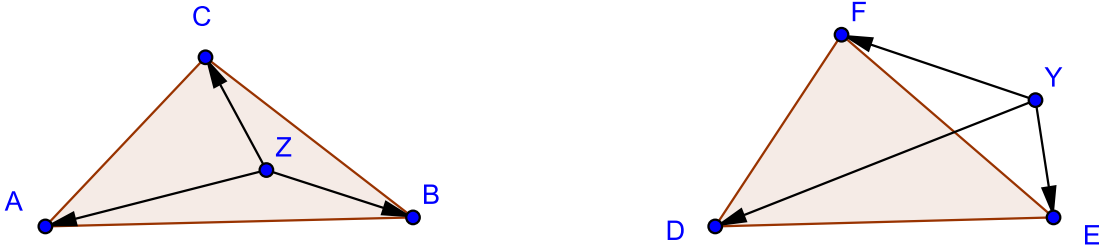


FIGURE 15. The cases “Inside” and “Outside”

“Inside” implies that  $g$  has a critical point by the standard theory of continuous selections theorem 2.2 in [APS]. Note that this means that  $x$  must be the (unique) intersection point of  $\text{Pow}(\alpha) \cap \text{Del}(\alpha)$ ; both sets lie in orthogonal linear subspaces of complementary dimension. Again compare this with the situation in section 2.2.

Using the techniques of [JS] one can see that “Outside” implies that  $g$  is regular at  $x$ .

The case “Border”, which is not covered by the general theory, we will treat it below. It should be noted that no general statements can be made about this case, but distance functions are special, see also [Gr], and for them some conclusions can be drawn.

Consider the Delaunay tessellation (dual to the power diagram). In the special case of the Euclidean distance function we have defined in section 2 a poset of active simplices in the Delaunay tessellation. They were defined using the critical points of  $\min g_i$ . We repeat the procedure for the power distance function.

Also, for a polyhedron  $P$  in  $\mathbb{R}^{n+1}$  the relative interior is the interior of the polyhedron as a subset of the affine span  $\text{Aff}(P)$  of  $P$ . If  $\dim \text{CH}(\alpha) > 0$  then put

$$(6) \quad c(\alpha) = \text{Sep}(\alpha) \cap \text{Aff}(\alpha)$$

where  $\text{Sep}(\alpha)$  is defined as

$$\text{Sep}(\alpha) = \{x \in \mathbb{R}^n \mid \forall i, j \in \alpha \quad \forall k \ni \alpha : f_i(x) = f_j(x) \neq f_k(x)\}$$

For a vertex put  $c(\{i\}) = P_i$ . Recall that for a convex set  $A$  a point  $x$  is contained in the relative interior of  $A$  if  $x$  is an interior point of  $A$  relative to the affine span  $\text{Aff}(A)$  of  $A$ .

**DEFINITION 7.** *We call the cell in the Delaunay tessellation active or critical if*

- $c(\alpha)$  is contained in the relative interior  $\text{Interior}(\text{CH}(\alpha))$  of  $\text{CH}(\alpha)$ , and
- $g(c(\alpha)) = g_i(c(\alpha))$  for all  $P_i \in \alpha$  and  $g(c(\alpha)) < g_j(c(\alpha))$  for all  $P_j \notin \alpha$ .

With this definition it might well happen that (in contrast with the Voronoi case) a vertex is not active. Here is a typical counter intuitive example. Take three points, say  $P_1 = (-1, 0)$ ,  $P_2 = (1, 1)$  and  $P_3 = (1, -1)$ . Then place a large circle around  $P_1$ :  $r_1 = 5$ . Place two smaller circles around  $P_2$  and  $P_3$ :  $r_2 = \sqrt{\frac{3}{4}}$  and  $r_3 = \sqrt{\frac{5}{6}}$ . If we look from below at the graph of  $\min g_i$  we see a picture alike the one in figure 16.

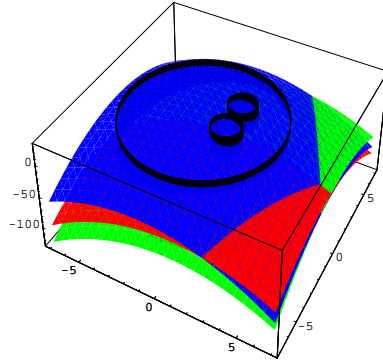


FIGURE 16. Typical counterintuitive example

**DEFINITION 8.** *The Morse poset of  $\{(P_i, w_i)\}_{i=1, \dots, N}$  consists of the active subsets of the Delaunay tessellation.*

Below we'll use the notation:

$$g_\alpha(x) = \min_{i \in \alpha} g_i(x) \quad \text{and} \quad f_\alpha(x) = \max_{i \in \alpha} f_i(x)$$

**THEOREM 7.** *There is a one to one correspondence between critical points of  $\min_i g_i$  and active cells in the Delaunay tessellation. An active cell of dimension  $d$  corresponds to a critical point of index  $d$ .*

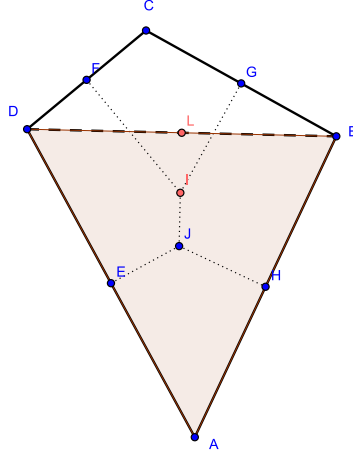


FIGURE 17. Morse poset, consisting of four 0-cells, four 1-cells and one 2-cell.

*Proof.* We will first rule out the case where  $d = 0$ . Because the functions  $g_i$  are all convex with minima at their respective vertices, a non-degenerate minimum can only occur on a vertex and the vertex will be active. Conversely, if a vertex  $P_i$  is active, we will have  $g_j(P_i) > g_i(P_i)$  for all  $j \neq i$ . And hence  $g$  will have a non-degenerate minimum there.

From now on assume that  $d > 0$ .

Let us again have  $x$  as in equation 5. Note that equation 5 implies an open condition: in a neighborhood  $x$  in  $\mathbb{R}^n$  the function  $g$  is entirely determined by the functions  $g_i$ , with  $i \in \alpha$ . Rephrasing that: there is a neighborhood  $U$  of  $x$  in  $\mathbb{R}^n$  such that  $g|_U = g_\alpha|_U$ .

As a consequence,  $g$  will have a critical point of index  $d$  at  $x$  if and only if  $g_\alpha$  has a critical point of index  $d$  at  $x$ . We consider again the three cases “Inside”, “Outside” and “Border” defined above. “Inside” implies that  $x = c(\alpha)$ , and hence  $\alpha$  is active and  $g$  has a critical point of index  $d = \dim(\alpha)$  at  $c(\alpha)$ . In more detail: choose coordinates  $y = (x_1, \dots, x_d)$  and  $z = (x_{d+1}, \dots, x_n)$ , such that  $\text{Aff}(\alpha)$  is defined by  $x_1 = \dots = x_d = 0$  and  $\text{Sep}(\alpha)$  is defined by  $x_{d+1} = \dots = x_n = 0$ . Next:

$$\begin{aligned} g_\alpha(x) &= \min_{i \in \alpha} g_i(x) = \min_{i \in \alpha} (1/2 \|y - P_i\|^2 - \frac{1}{2} w_i + \frac{1}{2} \|z\|^2) = \\ &= \min_{i \in \alpha} (1/2 \|y - P_i\|^2 - \frac{1}{2} w_i) + \frac{1}{2} \|z\|^2 \end{aligned}$$

So we have separation of variables. The first term defines a maximum in the origin of  $\mathbb{R}^d$  and is equivalent to  $-\frac{1}{2} \|y\|^2 + C$ . So  $g$  is equivalent to the standard Morse function of index  $d$ .

As we remarked above “Outside” implies that  $g$  is regular at  $x$ . Let us concentrate on the case “Border”. We have seen that  $\partial g(x)$  is a polyhedron spanned up by the vertices in  $\alpha$ .

Let  $\beta$  be the smallest face of  $\alpha$  such that  $x \in \text{CH}(\beta)$ . We have that  $x \in \text{CH}(\beta) \subset \text{Aff}(\beta)$ , and  $x \in \text{Pow}(\alpha) \subset \text{Pow}(\beta)$ . It follows that  $x = c(\beta) = c(\alpha)$ . We thus have to look at the level sets of  $g_\alpha$  near  $x = c(\beta) = c(\alpha)$ .

We claim that they are topologically equivalent (i.e. homeomorphic) to the level sets of a linear function.

In fact we can restrict attention to the behavior of  $g_\alpha$  on  $\text{Aff}(\alpha)$ . On the directions transversal to  $\text{Aff}(\alpha)$  and passing through  $c(\alpha)$   $g_\alpha$  is just a parabola with a minimum at  $c(\alpha)$ .

But when we restrict to  $\text{Aff}(\alpha)$  the only singularity  $g_\alpha$  can have at  $c(\alpha)$  is a maximum because  $g_\alpha$  attains its maximal value on  $\text{Del}(\alpha)$  at  $c(\alpha)$ . We thus have to prove that  $g_{\alpha|\text{Aff}(\alpha)}$  does not have a local maximum at  $c(\alpha)$ .

On  $\text{Pow}(\beta)$ , whose only point of intersection with  $\text{Pow}(\alpha)$  is  $c(\alpha)$ , we will have that  $g_{\alpha|\text{Aff}(\alpha)} \geq g(c(\alpha))$ . In fact on  $\text{Pow}(\beta)$  the value of  $g_\alpha$  will “wander off to infinity”. Hence  $g_{\alpha|\text{Aff}(\alpha)}$  cannot have a local maximum at  $c(\alpha)$ .  $\square$

**4.3. Morse formula.** We have the following Morse formula for the power distance function.

**THEOREM 8.** *Let  $s_i$  be the number of critical points of index  $i$  of  $g$ . We have:*

$$\sum (-1)^i s_i = 1$$

*Proof.*  $g$  is a topological Morse function. In that case, as  $t$  grows,  $g$  passes through a number of non-degenerate critical values. When  $g$  passes a critical value of index  $i$ , an  $i$ -cell gets attached [Mi1]. In between we apply the (topological) regular interval theorem. For each intermediate function value  $t$  we have therefore :

$$\chi(\{g(x) \leq t\}) = \sum (-1)^i s_i(t)$$

$\square$

Finally we remark that though power diagrams are affinely defined, activity is not retained under affine volume preserving linear transformations. Through such transformations the power diagram and its dual Delaunay tessellation do not change. The Morse poset though, can change drastically after an affine transformation.

## 5. DISCRETE MORSE THEORY

**5.1. Introduction.** As seen before the Morse poset is a subset of the Delaunay tessellation. There is a natural function on this poset, which describes the order of cell attaching: give each active cell the value of  $g$  in the critical point. An obvious question is how to extend this function to the full Delaunay tessellation. In this way one enters the framework of Forman’s discrete Morse theory. A very good introduction to that subject is [Fo2]. Descriptions of the theory exist in several categories, the most general is CW-complexes, cf. [Fo1]. More common and more accessible for an outsider is the description for simplicial complexes. We prefer to work inside the polyhedral category and avoid the CW-description.

Forman considers a function  $h$  on all cells of a simplicial complex, satisfying certain properties (see (7) and (8) below). He also considers the concept of critical or active cell. Following the evolution of values of  $h$  gives a protocol for constructing the simplicial

complex from a set of points. This works in such a way, that non-critical cells are attached in pairs and do not change the topology, while critical cells are attached separately and therefore change the topology.

In section 2.5 we have described how to proceed from the distance function  $g$  to a discrete Morse function that describes topology and shape in a convenient way. In general there are two problems for the extension of our distance function  $g$  to a discrete Morse function  $h$ :

- The Delaunay tessellation is not always a simplicial complex. This already happens in the plane.
- Some geometric defined candidates for  $h$  do not always satisfy the Forman conditions. This is related to the fact that, unlike Morse functions on a manifold, Forman discrete Morse functions are not dense in the set of all functions on a simplicial complex.

We will deal with both these issues and end up in section 6 with a discrete Morse function  $h$ , which extends  $g$ .

**5.2. Morse functions on Delaunay tessellation.** We first give the definition of a discrete Morse function and show next that the Delaunay tessellation has the property that for every two faces  $\alpha \subset \gamma$  with  $2 + \dim(\alpha) = \dim(\gamma)$  there are two faces  $\beta$  of the Delaunay tessellation in between  $\alpha$  and  $\gamma$ . This property will be important for constructing the discrete Morse function.

Let  $\mathcal{T}$  be a polyhedral subdivision.

**DEFINITION 9.** *A function  $h: \mathcal{T} \rightarrow \mathbb{R}$  is called a Forman discrete Morse function if for all  $\beta \in \mathcal{T}$*

$$(7) \quad \#\{\alpha \in \mathcal{T} \mid 1 + \dim(\alpha) = \dim(\beta) \ \alpha \subset \beta \ h(\alpha) \geq h(\beta)\} \leq 1$$

and

$$(8) \quad \#\{\alpha \in \mathcal{T} \mid \dim(\alpha) = 1 + \dim(\beta) \ \beta \subset \alpha \ h(\alpha) \leq h(\beta)\} \leq 1$$

*In case both numbers are zero for some  $\beta \in \mathcal{T}$ ,  $\beta$  is called critical.*

**EXAMPLE 2.** *In figure 18 we show a discrete Morse function. The values are indicated by numbers. Since they are choosen all different, we also can use them to indicate the faces. The critical faces are:*

- *0-dimensional: 1,2,4,6,10,11;*
- *1-dimensional: 3,5,14,15,16,17;*
- *2-dimensional: 18*

*Non critical faces occur in the following pairs: (8,9) and (12,13).*

*If one interchanges the labels 3 and 1 then we don't satisfy the definition of discrete Morse function.*

We define a Morse poset of a discrete Morse function  $h$  as the set of critical faces of  $h$ .



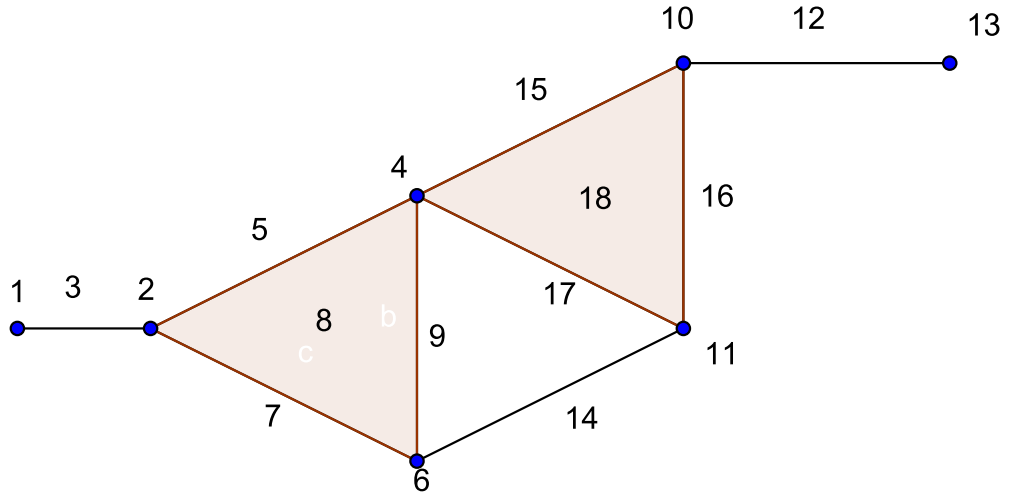
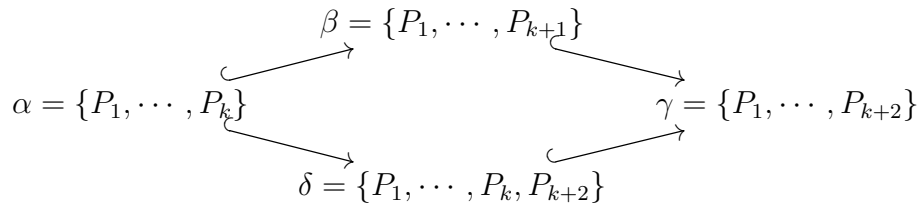


FIGURE 18. A discrete Morse function

If the power diagram  $\mathcal{T}$  is in general position then we know that it is a simplicial complex. Discrete Morse function on a simplicial complex have a very nice property, see lemma 2.6 in [Fo1]. If  $\alpha$  is a face of  $\beta$  and  $\beta$  is a face of  $\gamma$ . Label the vertices as follows:

$$\alpha = \{P_1, \dots, P_k\} \quad \beta = \{P_1, \dots, P_{k+1}\} \quad \gamma = \{P_1, \dots, P_{k+2}\}$$

Because we are dealing with a simplicial complex there is another face between  $\alpha$  and  $\gamma$ :  $\delta = \{P_1, \dots, P_k, P_{k+2}\}$ :



Let  $f$  be a discrete Morse function on the simplicial complex. Suppose that  $f(\alpha) \geq f(\beta) \geq f(\gamma)$ , that is both (7) and (8) hold. We also have  $f(\alpha) < f(\delta) < f(\gamma)$ , or

$$f(\gamma) > f(\delta) > f(\alpha) \geq f(\beta) \geq f(\gamma)$$

This is a contradiction, so we see that on simplicial complexes at most one (7) and (8) can hold.

However this argument is not restricted to simplicial complexes. All that is needed is that if  $\alpha$  and  $\gamma$  are two cells with  $\alpha \subset \gamma$  and  $2 + \dim \alpha = \dim \gamma$  then there are at least two cells in between  $\alpha$  and  $\gamma$ .

**THEOREM 9.** *Between any two cells  $\alpha$  and  $\gamma$  of a Delaunay tessellation with  $2 + \dim \alpha = \dim \gamma$  and  $\alpha \subset \gamma$  there are  $\beta_1$  and  $\beta_2$ , both cells in the Delaunay tessellation, both having dimension  $1 + \dim \alpha$  such that  $\alpha \subset \beta_i \subset \gamma$ .*

*Proof.* Consider the cone  $\text{Cone}(\gamma, \alpha)$  of  $\gamma$  over  $\alpha$ :

$$\text{Cone}(\gamma, \alpha) \stackrel{\text{def}}{=} \{\beta \mid \alpha \subseteq \beta \subseteq \gamma\}$$

Intersect that cone with the  $n - k + 1$  dimensional plane through zero and orthogonal to the  $k - 1$ -dimensional plane affinely spanned by  $\alpha$ . The intersection is a cone in the two dimensional plane. It has two extremal vectors  $\xi_1$  and  $\xi_2$ . These correspond to the faces  $\beta_1$  and  $\beta_2$  we were looking for.  $\square$

Hence even if the Delaunay tessellation is not simplicial, then we still have that not both (7) and (8) can hold.

**LEMMA 1.** *For a Delaunay tessellation with a discrete Morse function, then for any cell  $\beta$ , either:*

$$(9) \quad \#\{\alpha \in \mathcal{T} \mid 1 + \dim(\alpha) = \dim(\beta) \ \alpha \subset \beta \ h(\alpha) \geq h(\beta)\} = 0$$

or

$$(10) \quad \#\{\alpha \in \mathcal{T} \mid \dim(\alpha) = 1 + \dim(\beta) \ \beta \subset \alpha \ h(\alpha) \leq h(\beta)\} = 0 .$$

This will play a crucial role in the next section.

**5.3. Discrete vector fields.** On any coherent triangulation there exists a discrete Morse function:  $h: \alpha \mapsto \dim \alpha$ . But this function has all cells critical! The construction of discrete Morse functions with less critical points (even a minimal number), or prescribed values on certain cells is more delicate. As an example, in [KKM] one starts with assigning function values to vertices of a simplicial complex. They construct an algorithm for extension of a function on the vertices of a simplicial complex to a discrete Morse function on all cells of simplicial complex. We consider an other extension problem. The construction is rather involved and both [KKM] and we below use the concept of discrete gradient vector field from [Fo1].

Let us have a discrete Morse function  $h$  on the coherent triangulation. The (discrete) gradient of  $h$  consists (by definition) of arrows  $\alpha \rightarrow \beta$  between cells of adjacent dimensions, drawn when  $\alpha \subset \beta$  and  $h(\alpha) \geq h(\beta)$ . These cells can only occur in pairs, which are

disjoint. Keeping in mind the values of  $h$  we call  $\alpha$  *up* and  $\beta$  *down*. The remaining cells are all critical. In general such a collection of arrows is called a *discrete vector field*. A  $V$ -path is a sequence of arrows such that the cell pointed to contains a second cell that points to another one, of higher dimension. A *closed  $V$ -path* is a circular  $V$ -path as in equation (11). Theorem 3.5 in [Fo2] states that a discrete vector field is the gradient of a discrete Morse function if and only if it contains no closed  $V$ -paths.

$$(11) \quad \alpha_1 \rightarrow \beta_1 \supset \alpha_2 \rightarrow \beta_2 \supset \cdots \supset \alpha_k \rightarrow \beta_k \supset \alpha_1$$

The dual to the Delaunay tessellation, the power diagram, is also a polyhedral complex. Given a discrete Morse function  $\mathbf{g}$  on the Delaunay tessellation, clearly  $-\mathbf{g}$  is a discrete Morse function on the power diagram.

**5.4. Collapses.** In section 6 polyhedral collapses will play a significant role. To prepare for that section we recall some background information, see [Ma] and [Mi2] for more details.

Consider a polytope  $A$  with one of its codimension 1 faces  $F$ . We will delete the interior of  $A$  and the interior of the face  $F$ . The resulting space  $B$  is the union of the remaining codimension 1 faces of  $A$ . We call this process an elementary collapse of the polytope  $A$ . Notation  $A \searrow B$ .

Assume next that we have a space  $K$  tessellated by polytopes and that the polytope  $A$  is a  $k$ -cell of  $K$ . Assume that  $A$  has a free face  $F$ , i.e.  $F$  is only a face of  $A$  and not a face of any other cell. We repeat the construction and consider the space  $L$  obtained by deleting from  $K$  the interior of  $A$  and the interior of the face  $F$ . The transition from the space  $K$  to the space  $L$  is called an *elementary collapse*. Notation  $K \searrow L$ . A sequence of elementary collapses is called a *polyhedral collapse*.

Collapses are examples of deformation retractions in algebraic topology. Whitehead introduced simple homotopy theory. A basic reference for this is Milnor's paper [Mi2]. Two spaces are called  $s$ -homotopy equivalent if there is a sequence of elementary collapses and expansions to go from one space to the other. It is clear that any  $s$ -homotopy equivalence determines homotopy equivalence. The converse is not true. Whitehead's result states that there is an obstruction in the so-called Whitehead group of the fundamental group of the spaces. As soon as this obstruction is zero, which happens e.g. in simply connected spaces, both equivalences coincide.

Given an elementary collapse we could attach an arrow of a discrete vector field to the pair of cells. But also as soon as we have free faces, an arrow of a discrete vector field can be used for describing an elementary collapse. Note that in this way a  $V$ -path

$$\alpha_1 \rightarrow \beta_1 \supset \alpha_2 \rightarrow \beta_2 \supset \cdots \supset \alpha_k \rightarrow \beta_k$$

is naturally related to a  $s$ -homotopy equivalence:

$$L_1 \searrow L_2 \searrow \cdots \searrow L_k.$$

## 6. FROM MORSE POSET TO A DISCRETE VECTOR FIELD

**6.1. Introduction.** In this section we will construct the discrete Morse function on the Delaunay tessellation from the power distance function  $g$  defined in (1):

**THEOREM 10.** *On  $\text{Del}(\{P_1, \dots, P_N\})$  there exists a discrete Morse function  $h$  such that the Morse poset of  $h$  equals the Morse poset of  $g(x) = \min_{1 \leq i \leq N} g_i(x)$ .*

In fact we will not construct  $h$  directly. Instead we will construct a discrete vector field without closed  $V$ -paths.

We will use three different types of cells: *active*, *up* and *down*. The important difference with the gradient vector field above is that up-cells and down-cells no longer will occur in pairs, but up-cells can be coupled to several down-cells (of lower dimensions).

In the construction below the power center  $c(\alpha)$  will play an important role.

First recall definition 7: The cell  $\alpha$  in the Delaunay tessellation is *active* or *critical* if

- $c(\alpha)$  is contained in the relative interior  $\text{Interior}(\text{CH}(\alpha))$  of  $\text{CH}(\alpha)$ , and
- $g(c(\alpha)) = g_i(c(\alpha))$  for all  $P_i \in \alpha$  and  $g(c(\alpha)) < g_j(c(\alpha))$  for all  $P_j \notin \alpha$ .

A face  $\alpha$  can be non-active for one of two reasons

Down: The separator  $\text{Sep}(\alpha)$  can lie outside  $\text{Interior}(\text{CH}(\alpha))$ , or if that is not the case:

Up: Some point  $P_i \in \{P_1, \dots, P_N\} \setminus \alpha$  can lie closer to  $c(\alpha)$  than the points in  $\alpha$ , i.e.

$$(12) \quad g_i(c(\alpha)) \leq g_j(c(\alpha)) \quad \forall j \in \alpha$$

NB. We have identified  $\alpha$  with its index set.

To illustrate these concepts we refer the reader to figure 20. In that figure the cell  $\{P_1, P_2\}$  is not active for the “Up” reason. The cell  $\{P_1, P_2, P_3, P_4\}$  is not active. It cannot be not active for the “Up” reason, because there is no cell in which it is contained. Indeed  $\{P_1, P_2, P_3, P_4\}$  is not active for the “Down” reason. The separator  $\text{Sep}(P_1, P_2, P_3, P_4)$  is just  $c(P_1, P_2, P_3, P_4)$  and it clearly lies outside the tetrahedron.

The reader is encouraged to repeat this exercise for figure 16, which we have also drawn in figure 22.

Next we show two properties:

- Suppose that  $\alpha$  is not active for the “Down” reason. Then in the case of Voronoi diagrams  $\alpha$  cannot be a vertex or an edge. In general with power diagrams  $\alpha$  cannot be a vertex.
- Suppose that  $\alpha$  is not active for the “Up” reason and that  $\dim \text{Del}(\alpha) = n$ . Then we have

$$\{c(\alpha)\} = \bigcap_{j \in \alpha} \text{Pow}(\{P_j\}):$$

we cannot have inequality (12). We conclude that no  $\alpha$ , not active for the “Up” reason has  $\dim \text{Del}(\alpha) = n$ .

**6.2. Investigating the up-down structure.** We start by showing that for every face, not active for the “Down” reason, there is a unique lower dimensional cell not active for the “Up” reason. Then we construct for each face not active for the “Up” reason a part of the discrete vector field.

**LEMMA 2.** *Let  $\beta \in \text{Del}(\{P_1, \dots, P_N\})$  be a face not active for the “Down” reason. Then the closest point to  $\text{CH}(\beta)$  from  $c(\beta)$  is  $c(\alpha)$  for some proper face  $\alpha$  of  $\beta$ . At  $c(\alpha)$  we have*

$$(13) \quad g_j(c(\alpha)) \leq g_\alpha(c(\alpha)) \quad \forall j \in \beta \setminus \alpha$$

*Hence  $\alpha$  is not active for the “Up” reason. Conversely if (13) holds for  $\beta \supset \alpha$  then  $\beta$  is not active for the “Down” reason.*

*Proof.* We start with “ $\Rightarrow$ ”.

A special case we first have to handle is when  $c(\beta)$  lies on the relative boundary of  $\text{CH}(\beta)$ . This means that  $c(\beta) \in \text{CH}(\alpha)$  for some proper face  $\alpha$  of  $\beta$ . Because  $\text{Sep}(\beta) \subset \text{Sep}(\alpha)$  it follows that  $c(\beta) = c(\alpha)$ . Equation (13) follows automatically.

Now we can safely assume that the distance from  $c(\beta)$  to  $\text{CH}(\beta)$  is  $> 0$ . Denote  $y$  the closest point on  $\text{CH}(\beta)$  from  $c(\beta)$ . If  $\alpha$  is a vertex we are done, so suppose that  $\alpha$  is not a vertex. The line from  $y$  to  $c(\beta)$  is orthogonal to  $\text{Aff}(\alpha)$  and hence parallel to  $\text{Sep}(\alpha)$ . Clearly  $c(\beta)$  lies in  $\text{Sep}(\alpha)$ . So  $y$  also lies in  $\text{Sep}(\alpha)$ . But  $y$  also lies in  $\text{Aff}(\alpha)$ . So, by the definition of  $c(\alpha)$  in equation (6) we have that  $y = c(\alpha)$ .

Because  $\text{CH}(\beta)$  is a convex set the hyperplane with normal  $c(\beta) - c(\alpha)$  passing through  $c(\alpha)$  separates  $\text{Interior}(\text{CH}(\beta))$  from  $c(\beta)$ . Thus for a vertex  $P_k$  of  $\beta$  the angle  $P_k$  to  $c(\alpha)$  to  $c(\beta)$  must be obtuse. Consequently:

$$(14) \quad \|c(\beta) - P_k\|^2 \geq \|c(\beta) - c(\alpha)\|^2 + \|c(\alpha) - P_k\|^2$$

if  $P_k$  is a vertex in  $\beta \supset \alpha$ . By the Pythagoras theorem, equality holds if  $k \in \alpha$ :

$$(15) \quad \|c(\beta) - P_k\|^2 = \|c(\beta) - c(\alpha)\|^2 + \|c(\alpha) - P_k\|^2$$

Then equation (14) becomes, taking the factor  $\frac{1}{2}$  we used in the definition of  $g$  in equation (1) into account:

$$(16) \quad g_k(c(\beta)) \geq \frac{1}{2} \|c(\beta) - c(\alpha)\|^2 + g_k(c(\alpha)) \quad k \in \beta \setminus \alpha$$

Again, equality holds when  $k \in \alpha$ . Putting this together we get (13), and we see that  $\alpha$  is not active for the “Up” reason.

Next do the “ $\Leftarrow$ ” part. We assume (13) and  $\alpha \subset \beta$ . From (13) we get for  $j \in \beta \setminus \alpha$ :

$$(17) \quad g_j(c(\alpha)) + \frac{1}{2} \|c(\beta) - c(\alpha)\|^2 \leq g_\alpha(c(\alpha)) + \frac{1}{2} \|c(\beta) - c(\alpha)\|^2 = g_\alpha(c(\beta)) = g_j(c(\beta))$$

The special case to handle first is where equality holds in (17). Then  $c(\beta) = c(\alpha)$  and so  $c(\beta)$  is not an element of the relative interior  $\text{Interior}(\text{CH}(\beta))$ . So  $\beta$  is not active for the “Down” reason.

Now we can safely assume strict inequality in (17). The simplest case is a  $\beta$  for which  $\beta = \alpha \cup \{j\}$ . The three points  $P_j$ ,  $c(\beta)$  and  $c(\alpha)$  all lie in  $\text{Aff}(\beta)$ . From (17) we get (14) with strict inequality. The line segment from  $c(\alpha)$  to  $c(\beta)$  is thus an outward normal to

$\text{CH}(\beta)$  in  $\text{Aff}(\beta)$ . Consequently  $\beta$  is not active for the “Down” reason. The general case is similar.  $\square$

**6.3. Defining the up-sets.** Let again  $\alpha$  be not active for the “Up” reason. Denote  $K$  the set of indices for which (12) holds. Denote  $\text{Up}(\alpha)$  the set of simplices:

$$(18) \quad \text{Up}(\alpha) = \{\beta \in \text{Del}(\{P_1, \dots, P_N\}) \mid \alpha \subset \beta \subset \alpha \cup K\}$$

Lemma 2 characterizes the elements of  $\text{Up}(\alpha)$  as those  $\beta \supset \alpha$  for which  $c(\alpha)$  is the closest point on  $\text{CH}(\beta)$  from  $c(\beta)$ . The complement of the Morse poset is divided into different subsets  $\text{Up}(\alpha)$ , one for each face not active for the “Up” reason. We need to prove that each  $\text{Up}(\alpha)$  can be filled up with a discrete vector field.

We will establish another criterion (in terms of power sets) for which a  $\beta \in \text{Del}(\{P_1, \dots, P_N\})$  with  $\alpha \subset \beta$  is an element of  $\text{Up}(\alpha)$ . Take the point  $c(\alpha)$  outside the polytope  $\text{Pow}(\alpha)$  in  $\text{Sep}(\alpha)$  and consider the faces of  $\text{Pow}(\alpha)$  for which the outward pointing normal makes an angle smaller than 90 degrees with  $x - c(\alpha)$ , where  $x$  be a point in the interior of  $\text{Pow}(\beta)$ . Then we get a number of faces  $\beta_1, \dots, \beta_l$  in the Delaunay tessellation that we see as faces  $\text{Pow}(\beta_1), \dots, \text{Pow}(\beta_l)$  on the relative boundary  $\partial(\text{Pow}(\alpha))$  of  $\text{Pow}(\alpha)$ . This is illustrated in figure 19 and 20. A precise formulation is contained in the following lemma.

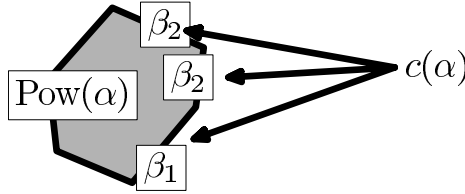


FIGURE 19. View from  $c(\alpha)$  to  $\text{Pow}(\alpha)$  inside the plane  $\text{Aff}(\alpha)$ . In this case  $\text{Up}(\alpha)$  contains  $\beta_1, \beta_2$  and  $\beta_3$ . Lemma 3 shows that this is equivalent to their power cells being “visible” from  $c(\alpha)$ .

**LEMMA 3.** *Let  $\beta \supset \alpha$  be an element of  $\text{Del}(\{P_1, \dots, P_N\})$ ,  $\alpha$  not active for the “Up” reason. Let  $x$  be a point in the interior of  $\text{Pow}(\beta)$ . If, either  $x = c(\alpha)$ , or*

- (1) *the line through  $x$  and  $c(\alpha)$  intersects  $\text{Pow}(\alpha)$  in a segment, and*
- (2) *the segment  $[x, c(\alpha)]$  contains no point of the interior of  $\text{Pow}(\alpha)$*

*then  $\beta \in \text{Up}(\alpha)$ . Conversely, if  $\beta \in \text{Up}(\alpha)$  and  $x$  lies in the interior of  $\text{Pow}(\beta)$  then 1 and 2 hold, or  $x = c(\alpha)$ .*

*Proof.* We first need to treat the case  $x = c(\alpha)$ . In that case  $c(\alpha)$  lies on the relative boundary of  $\text{Pow}(\alpha)$ . So  $x \in \text{Pow}(\beta)$ ,  $\beta = \alpha \cup I$ . And  $f_j(c(\alpha)) = f_\alpha(c(\alpha))$ , for all  $j \in I$ . (note that we use here the affine functions from section 3.) Obviously  $\text{Up}(\alpha)$  consists exactly of all those  $\gamma \in \text{Del}(\{P_1, \dots, P_N\})$  with

$$\alpha \subseteq \gamma \subseteq \beta = \alpha \cup I$$

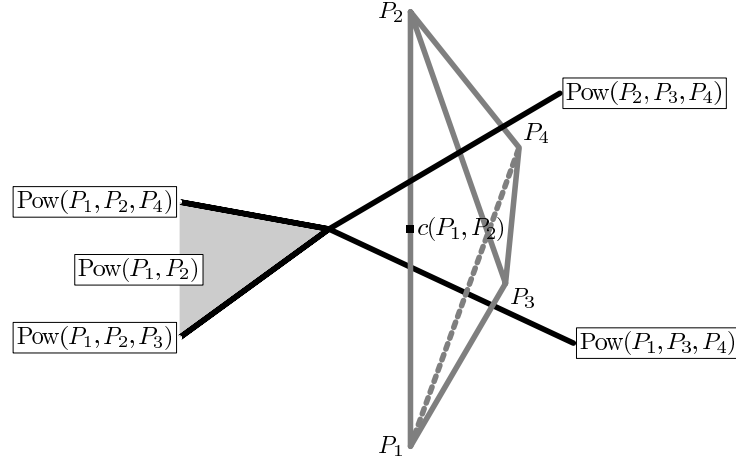


FIGURE 20. Second, less schematic example, of  $\text{Up}(\alpha)$ . In this example  $\text{Up}(P_1, P_2)$  consists of  $\{P_1, P_2\}$ ,  $\{P_1, P_2, P_3\}$ ,  $\{P_1, P_2, P_4\}$  and  $\{P_1, P_2, P_3, P_4\}$ . From  $c(P_1, P_2)$  we can see exactly the power cells of those simplices that lie in  $\text{Up}(P_1, P_2)$ .

Now we can assume  $x \neq c(\alpha)$ . Again  $x$  lies on the relative boundary of  $\text{Pow}(\alpha)$  and  $\beta = \alpha \cup I$  for some maximal set  $I$ . We put  $x_t = tx + (1-t)c(\alpha)$ . Hence  $x_1 = x$  and  $x_0 = c(\alpha)$ . It also follows for  $j \in I$

$$f_j(x_t) = tf_j(x) + (1-t)f_j(c(\alpha)) = tf_\alpha(x) + (1-t)f_j(c(\alpha))$$

and thus

$$f_j(x_t) - f_\alpha(x_t) = (1-t)(f_j(c(\alpha)) - f_\alpha(c(\alpha)))$$

Now we have

$$f_j(c(\alpha)) \geq f_\alpha(c(\alpha)) \Leftrightarrow \exists t > 1 : f_j(x_t) \leq f_\alpha(x_t)$$

So that

$$\exists t > 1 \ x_t \in \text{Pow}(\alpha) \Rightarrow f_j(c(\alpha)) \geq f_\alpha(c(\alpha))$$

And this is exactly what we needed to prove.

For the converse suppose that  $\beta \supset \alpha$ , and  $\alpha$  not active for the “Up” reason, but that 1 and 2 do not hold.

The only point of  $\text{Pow}(\alpha)$  on the line through  $x$  and  $c(\alpha)$  is  $x$ . It follows that  $\beta \setminus \alpha$  contains more than one index, i.e.  $\beta = \alpha \cup \{j_1, \dots, j_r\}$  with  $r \geq 2$ . In a sufficiently small neighborhood of  $x$  the half spaces  $H_i = \{f_{j_i} \leq f_\alpha\}$  define  $\text{Pow}(\alpha)$  as a polyhedron in  $\text{Sep}(\alpha)$ . Because  $\{x_t \mid t \in \mathbb{R}\}$  touches  $\text{Pow}(\alpha)$  there exist an index  $k$ , say  $k = j_1$ , and a  $t < 1$  such that  $f_j(x_t) - f_\alpha(x_t)$  and hence  $f_k(c(\alpha)) < f_\alpha(c(\alpha))$ . And so  $\beta \supset \alpha$  is not an element of  $\text{Up}(\alpha)$ .  $\square$

**6.4. Construction of the discrete vector field.** Let  $\alpha$  be not active for the “Up” reason. Hence  $c(\alpha)$  lie outside  $\text{Pow}(\alpha)$ . We will consider  $c(\alpha)$  as center of a system of rays. As seen above this system of rays defines a cone, which meets the boundary  $\partial \text{Pow}(\alpha)$  exactly in  $\text{Front}(\alpha)$ , i.e. those  $\text{Pow}(\beta)$ , where  $\beta$  in  $\text{Up}(\alpha)$  is different from  $\alpha$ .

This  $\text{Front}(\alpha)$  is part of  $\partial \text{Pow}(\alpha)$  and is contractible, since  $\text{Pow}(\alpha)$  is convex.

We can use the extension of rays to define a deformation retract to the back side:

$$\text{Pow}(\alpha) \longrightarrow \text{Back}(\alpha) := \overline{\text{Pow}(\alpha) - \text{Front}(\alpha)}$$

NB. In case  $\text{Pow}(\alpha)$  is not bounded there is a small complication, which can be solved by adding some extra points, that do not effect the situation in  $\text{Up}(\alpha)$ .

Since all spaces we consider are contractible, this deformation retraction can be realized by elementary collapses. This a different way to express, that there exists a discrete vector field on  $\text{Pow}(\text{Up}(\alpha))$ . Due to the contractibility this vector field has no closed  $V$ -paths.

By duality there exists a discrete vector field without closed  $V$ -paths on  $\text{Up}(\alpha)$ .

We conclude that the complement of the Morse poset can be divided into separate parts  $\text{Up}(\alpha)$ , for all up-cells  $\alpha$  and on each  $\text{Up}(\alpha)$  we have defined a discrete vector field without closed  $V$ -paths. This defines a discrete vector field on  $\text{Del}(P_1, \dots, P_N)$  by “no-arrow” extension on the Morse poset. To show that we indeed get a discrete Morse function we need to prove one more thing: there should be no global closed  $V$ -path.

**6.5. No global  $V$ -loops.** Suppose that we have a closed  $V$ -path. Inside one  $\text{Up}(\alpha)$  there is no such closed  $V$ -path, so at some cell the  $V$ -path should jump from one  $\text{Up}(\gamma_1)$  to another  $\text{Up}(\gamma_2)$ , as in figure 21.

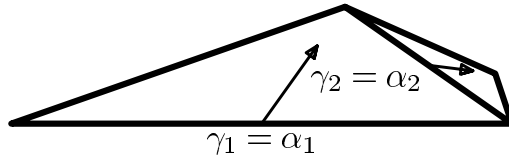


FIGURE 21. A  $V$ -path, with a jump from  $\text{Up}(\gamma_1)$  to  $\text{Up}(\gamma_2)$ .

**LEMMA 4.** *Suppose that we have a  $V$ -path that jumps from  $\text{Up}(\gamma_1)$  to  $\text{Up}(\gamma_2)$  as in equation (19).*

$$(19) \quad \begin{array}{l} \alpha_i \rightarrow \beta_i \quad \subset \text{Cone}(\gamma_1 \cup I_1, \gamma_1) \\ \cup \\ \alpha_{i+1} \rightarrow \beta_{i+1} \subset \text{Cone}(\gamma_2 \cup I_2, \gamma_2) \end{array}$$

Then  $g_{\gamma_1}(c(\gamma_1)) > g_{\gamma_2}(c(\gamma_2))$ .

*Proof.* Because  $\gamma_1$  is a proper subset of  $\gamma_1 \cup \gamma_2$  we see that:  $c(\gamma_1 \cup \gamma_2) \notin \text{Interior}(\text{CH}(\gamma_1 \cup \gamma_2))$ . The closest point to  $\text{CH}(\gamma_1 \cup \gamma_2)$  from  $c(\gamma_1 \cup \gamma_2)$  is  $c(\gamma_1)$ , as we have shown in lemma 2. In particular

$$(20) \quad \|c(\gamma_1 \cup \gamma_2) - c(\gamma_1)\|^2 < \|c(\gamma_1 \cup \gamma_2) - c(\gamma_2)\|^2$$

Here, the inequality is strict. The closest point is unique, because  $\text{CH}(\gamma_1 \cup \gamma_2)$  is convex.

For the reasons explained in the proof of lemma 2 we have

$$(21) \quad g_{\gamma_1 \cup \gamma_2}(c(\gamma_1 \cup \gamma_2)) = g_{\gamma_1}(c(\gamma_1 \cup \gamma_2)) = \frac{1}{2} \|c(\gamma_1 \cup \gamma_2) - c(\gamma_1)\|^2 + g_{\gamma_1}(c(\gamma_1))$$



The same identity holds with  $\gamma_1$  and  $\gamma_2$  exchanged, thus:

$$(22) \quad \frac{1}{2} \|c(\gamma_1 \cup \gamma_2) - c(\gamma_1)\|^2 + g_{\gamma_1}(c(\gamma_1)) = \frac{1}{2} \|c(\gamma_1 \cup \gamma_2) - c(\gamma_2)\|^2 + g_{\gamma_2}(c(\gamma_2))$$

Putting (20) and (22) together we get the desired result.  $\square$

Lemma 4 says that to each  $\text{Up}(\alpha)$  appearing in the  $V$ -path we can associate a number, and passing from one  $\text{Up}(\alpha)$  to another that number strictly decreases. Hence we can not have a closed  $V$ -path. The proof of theorem 10 is complete.

**6.6. Constructing the extension.** We constructed above a discrete Morse function with the same Morse poset as  $g$ . What is lost in the proof is a direct relation between  $g$  and the discrete Morse function that results from the discrete vector field we constructed. A good candidate for such a Morse function could be:

$$h : \mathfrak{g} \rightarrow \mathbb{R} ; \quad h(\beta) = \sup_{x \in \text{CH}(\beta)} g(x)$$

as a function on the Delaunay tessellation. Inspection of this function shows, that it is indeed critical on the Morse poset, but has constant values on all cells of a given  $\text{Up}(\alpha)$ . So it violates the rules of Morse functions as soon as  $\text{Up}(\alpha)$  contains more than two cells. We will use the discrete vector field on  $\text{Up}(\alpha)$  (defined above) to perturb these values. Remark that the vector field induces on  $\text{Up}(\alpha)$  a ‘potential function’; call it  $h_\alpha$ . Set  $h_\alpha(\beta) = 0$  as soon as  $\beta \notin \text{Up}(\alpha)$ . One has the freedom to scale  $h_\alpha$  such that it takes values in small interval around 0. The function

$$\hat{h} : \mathfrak{g} \rightarrow \mathbb{R} ; \quad \hat{h}(\beta) = \sup_{x \in \text{CH}(\beta)} g(x) + \sum_{\alpha \text{ up}} h_\alpha(\beta)$$

is a good extension as soon as the scaling is small enough. So we have :

**THEOREM 11.** *The function  $\hat{h}$  is a discrete Morse function, with the same Morse poset as  $g$  and which assigns to each element of the Morse poset the corresponding critical value of  $g$ .*

**REMARK 2.** *The above discussion shows that the vector field is not unique. The non-uniqueness only lies in the choice of the arrows possible in  $\text{Up}(\alpha)$ . It seems more natural to consider a single polyhedral collapse of  $\text{Up}(\alpha)$ . But Forman’s discrete Morse theory is ill equipped for dealing with bigger polyhedral collapses. One could also try to develop a generalization of discrete Morse theory in order to include these polyhedral collapses.*

## 7. EXAMPLES AND COMMENTS.

**7.1. Vertices that are not active.** Let us return to the counterintuitive example of figure 16. There the Morse poset is as in figure 22. In the picture we see three cones, consisting each of two faces in the simplest triangulation one can think of.

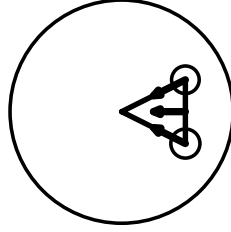


FIGURE 22. Morse poset and discrete vector field of figure 16

**7.2. 3 dimensional case.** In [SvM] we studied the Morse theory of a tetrahedron in  $\mathbb{R}^3$ . As we found, that for triangles in  $\mathbb{R}^2$  generically there are two different Morse posets, we showed that there are generically nine different Morse posets for the tetrahedron. To be more precise: theorem 12 tells us exactly the possible positions of critical points. The number  $s_i$  of critical point of index  $i$  are bounded by 4, 6, 4, 1 for index 0, 1, 2, 3 Moreover the Euler characteristic of  $\mathbb{R}^3$  is +1, so by Morse Formula:  $s_0 - s_1 + s_2 - s_3 = 1$  This gives a priori the following 9 possibilities:

$s_0$	$s_1$	$s_2$	$s_3$
4	6	4	1
4	5	3	1
4	4	2	1
4	3	1	1
4	2	0	1
4	6	3	0
4	5	2	0
4	4	1	0
4	3	0	0

But not all these will occur. Since we start with 4 vertices and the result should be a connected space, we need at least 3 saddle points of index 1. Hence, we cannot have (4, 2, 0, 1).

We list in figure 23 the (a priori) possible 1-skeletons of the Morse poset (also know as Gabriel graphs) for the above cases, they are the connected graphs with 4 vertices. Just as the case (4, 2, 0, 1) can not occur, we showed in [SvM] that the cases (4, 4, 2, 1)  $P$ , (4, 3, 1, 1)  $T$  and (4, 3, 1, 1)  $L$  do not occur.

**THEOREM 12.** *Up to affine bijections of a tetrahedron in  $\mathbb{R}^3$ , which send the Morse posets to each other, there are nine generic tetrahedra. They are uniquely described by the nine Gabriel graphs (4, 6, 4, 1), (4, 6, 3, 0), (4, 5, 3, 1), (4, 5, 2, 0), (4, 4, 2, 1)  $O$ , (4, 4, 1, 0)  $O$ , (4, 4, 1, 0)  $P$ , (4, 3, 0, 0)  $L$  and (4, 3, 0, 0)  $T$ , drawn in figure 23.*

The example 4300I is interesting, since it shows a polyhedral collapse. In figure 20 we have reproduced an example of such a tetrahedron. The face  $\{P_1, P_2\}$  is not active for the “Up” reason. In that case both  $\{P_1, P_2, P_3\}$  and  $\{P_1, P_2, P_4\}$  and  $\{P_1, P_2, P_3, P_4\}$  are not

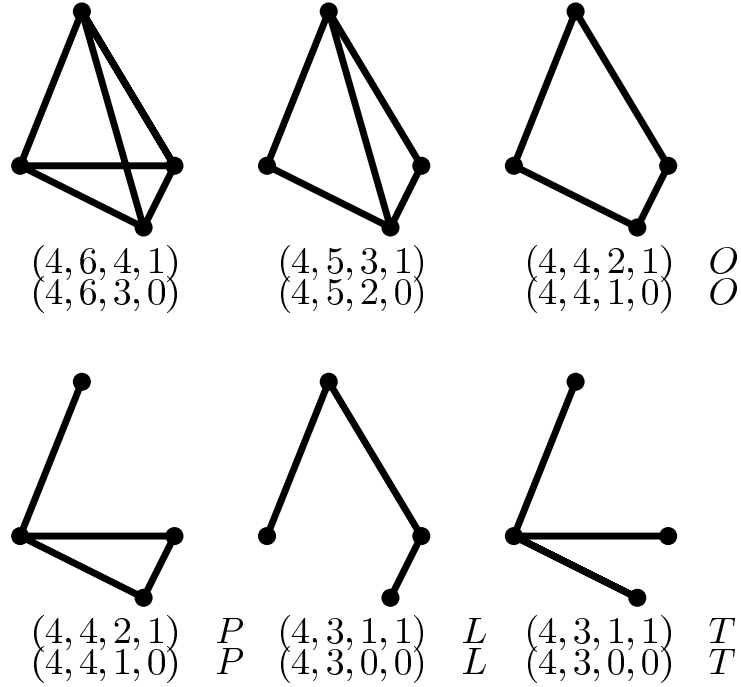


FIGURE 23. List of a priori possible Gabriel graphs. The vertices are the minima of the distance function. Each vertex of the tetrahedron  $\mathbb{T}$  is a minimum of  $d$ . There are no other minima. The edges of the graph are the index 1 critical points of the distance function. Not each midpoint of an edge of  $\mathbb{T}$  is an index 1 critical point of the distance function  $d$ . The graph (4410)  $O$  can be laid out so as to form the letter “O”. The names of the other graphs are chosen similarly.

active for the “Down” reason. There is one cone consisting of the polyhedral collapse:

$$\{P_1, P_4\} \rightarrow \{P_1, P_2, P_4\} \quad \{P_1, P_3, P_4\} \rightarrow \{P_1, P_2, P_3, P_4\}$$

The decomposition of that cone into arrows is not unique. We might just as well write

$$\{P_1, P_4\} \rightarrow \{P_1, P_3, P_4\} \quad \{P_1, P_2, P_4\} \rightarrow \{P_1, P_2, P_3, P_4\}$$

**7.3. 2 dimensional case.** In the same spirit we have the classification of all Morse posets of Voronoi diagrams for 4 points in the plane in [Si]. Unfortunately there were two cases missing, which are now included in figure 24.

**7.4. Enumerating all power diagrams and Voronoi diagrams.** The Morse poset is the discrete structure that encodes the flow of the distance function  $g(x) = \min_{1 \leq i \leq N} g_i(x)$ . It is unclear whether the problem of enumerating all power diagrams is equivalent to the problem of enumerating all coherent triangulations. That last problem is nicely solved using the secondary polytope, see [GKZ]. For many applications though a discrete structure describing a Voronoi diagram should contain more geometric information. The Morse

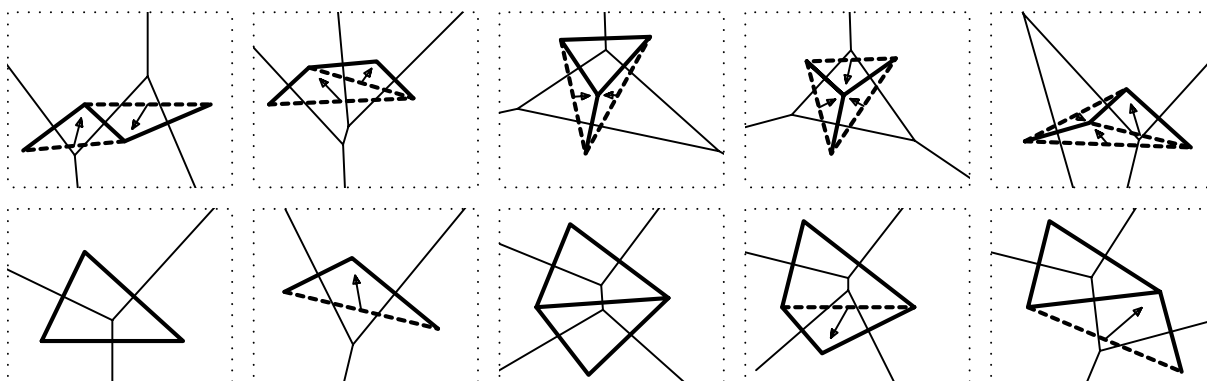


FIGURE 24. 3 and 4 points in  $\mathbb{R}^2$ : all Morse posets from Voronoi diagrams with the accompanying discrete vector fields

poset and the discrete vector field do exactly that. In figure 24 we see that there are 2 combinatorially different triangulations of four points in the plane. Taking into account the Morse poset yields 8 different cases.

#### REFERENCES

- [APS] A. A. Agrachev, D. Pallaschke, and S. Scholtes. On Morse theory for piecewise smooth functions. *J. Dynam. Control Systems*, 3(4):449–469, 1997.
- [Au1] F. Aurenhammer, *Voronoi Diagrams - A Survey of a Fundamental Geometric Data Structure*, ACM ComputingSurveys, Vol 23, p 345- 405 (1991).
- [Au2] F. Aurenhammer. Power diagrams: properties, algorithms and applications. *SIAM J. Comput.*, 16(1):78–96, 1987.
- [Bl] D. W. Blackett. *Elementary Topology*, Academic Press, 1982.
- [DFG] D. E. Diaconescu, B. Florea, and A. Grassi. Geometric transitions, del Pezzo surfaces and open string instantons. *Adv. Theor. Math. Phys.*, 6(4):643–702, 2002.
- [Ch] J. Cheeger. Critical Points of Distance Functions and Applications to Geometry In *Geometric Topology: recent developments*, Springer Lecture Notes, 1054,pp. 1-38, 1991.
- [Cl] F. H. Clarke. *Optimization and Nonsmooth Analysis*. SIAM, 1990
- [CL] F. Chazal and A. Lieutier. Topology guaranteeing manifold reconstruction using distance function to noisy data. In *SCG '06: Proceedings of the twenty-second annual symposium on Computational geometry*, pp. 112–118. ACM Press, 2006.
- [DGJ] T. K. Dey, J. Giesen and M. John. Alpha-shapes and flow shapes are homotopy equivalent. In *Proceedings of the Thirty-Fifth Annual ACM Symposium on Theory of Computing*, pp. 493–502, ACM, New York, 2003.
- [Ed1] H. Edelsbrunner. *Algorithms in Combinatorial Geometry*, volume 10 of *ATCS, Monographs on Computer Science* Springer Verlag, 1987.
- [Ed2] H. Edelsbrunner. The union of balls and its dual shape. In *SCG '93: Proceedings of the ninth annual symposium on Computational geometry*, pp. 218–231. ACM Press, 1993.
- [Ed3] H. Edelsbrunner. Surface reconstruction by wrapping finite sets in space. *Algorithms and combinatorics*, 25:379–404, 2003.
- [Fo1] R. Forman. Morse theory for cell complexes. *Adv. Math.*, 134(1):90–145, 1998.
- [Fo2] R. Forman. A user's guide to discrete Morse theory. *Sém. Lothar. Combin.*, 48:Art. B48c, 35 pp. (electronic), 2002.

- [GS] K. R. Gabriel and R. R. Sokal. A new statistical approach to geographic variation analysis. *Syst. Zoology*, 18:259-278, 1969.
- [Ga] A. Gathmann. Tropical algebraic geometry. *Jahresbericht der DMV*, 108(1):3-32, 2006.
- [GJ1] J. Giesen and M. John. Computing the Weighted Flow Complex In *Proceedings of the 8th International Fall Workshop Vision, Modelling and Visualization (VMV)* pp. 235-243, 2003
- [GJ2] J. Giesen and M. John. The flow complex: a data structure for geometric modeling. *Comput. Geom.* 39( 3): 178-190, 2008
- [GKZ] I. M. Gelfand, M. M. Kapranov, and A. V. Zelevinsky. *Discriminants, resultants, and multidimensional determinants*. Mathematics: Theory & Applications. Birkhäuser Boston Inc., Boston, MA, 1994.
- [GM] M. Goresky and R. MacPherson. *Stratified Morse Theory*, volume 14 of *Ergebnisse der Mathematik und ihrer Grenzgebiete; 3. Folge*. Springer Verlag, 1987.
- [Gr] K. Grove. Critical Point Theory for Distance Functions. In *Differential Geometry: Riemannian Geometry, Proceedings of Symposia in Pure Mathematics*, 54(3):357-385, 1993.
- [Hi] M. W. Hirsch. *Differential topology*, volume 33 of *Graduate Texts in Mathematics*. Springer Verlag, 1976.
- [Hö] L. Hörmander. *Notions of convexity*, volume 127 of *Progress in Mathematics*. Birkhäuser Boston Inc., Boston, MA, 1994.
- [JS] H.Th. Jongen and D. Pallaschke. On linearization and continuous selections of functions. *Optimization*, 19(3):343-353, 1988.
- [KKM] H. King, K. Knudson and N. Mramor. Generating discrete morse functions from point data. *Journal Experimental Mathematics* 14(4):435-444, 2005.
- [Ma] S. Matveev. *Algorithmic topology and classification of 3-manifolds*, volume 9 of *Algorithms and Computation in Mathematics*. Springer-Verlag, Berlin, 2003.
- [Mi1] J. Milnor. *Morse Theory*, Annals of Mathematics Studies 51, Princeton University Press 1963.
- [Mi2] J. Milnor. Whitehead torsion. *Bull. Amer. Math. Soc.*, 72:358-426, 1966.
- [Mo1] M. Morse. Topologically non-degenerate functions on a compact  $n$ -manifold  $M$ . *J. Analyse Math.*, 7:189-208, 1959.
- [Mo2] M. Morse.  $F$ -deformations and  $F$ -tractions *Proc. Nat. Acad. Sci. U.S.A.*, 70:1634-1635, 1973.
- [OBS] A. Okabe, B. Boots and K. Sugihara. *Spatial Tesselations, Concepts and Applications of Voronoi Diagrams*, Wiley series in probability and mathematical statistics, 1992.
- [PR] M. Passare and H. Rullgård. Amoebas, Monge-Ampère measures, and triangulations of the Newton polytope. *Duke Math. J.*, 121(3):481-507, 2004.
- [RST] J. Richter-Gebert, B. Sturmfels, and T. Theobald. First steps in tropical geometry. *arXiv.math*, AG.0306366:1-29, 2003.
- [Si] D. Siersma. Voronoi diagrams and Morse theory of the distance function. In *Geometry in Present Day Science*, 187-208. World Scientific, Singapore, 1999.
- [SvM] D. Siersma and M. van Manen. The nine Morse generic tetrahedra. *SIAM J. Discrete Math.*, 22(2):737-746, 2008
- [Ur] R. Urquhart. Graph theoretical clustering based on limited neighborhood sets *Pattern Recognition* 15(3):173-187, 1982.
- [Zi] G. M. Ziegler. *Lectures on polytopes*, volume 152 of *Graduate Texts in Mathematics*. Springer-Verlag, 1995.